RSC Advances

PAPER

View Article Online
View Journal | View Issue

Check for updates

Cite this: *RSC Adv.*, 2023, **13**, 10523

Synthesis of 3,4-dihydroisoquinolin-1(2*H*)-one derivatives and their antioomycete activity against the phytopathogen *Pythium recalcitrans*†

Delong Wang, ‡ Min Li,‡ Jing Li, Yali Fang * and Zhijia Zhang*

In an effort to exploit the bioactive natural scaffold 3,4-dihydroisoquinolin-1(2*H*)-one for plant disease management, 59 derivatives of this scaffold were synthesized using the Castagnoli–Cushman reaction. The results of bioassay indicated that their antioomycete activity against *Pythium recalcitrans* was superior to the antifungal activity against the other 6 phytopathogens. Compound **I23** showed the highest *in vitro* potency against *P. recalcitrans* with an EC_{50} value of 14 μM, which was higher than that of the commercial hymexazol (37.7 μM). Moreover, **I23** exhibited *in vivo* preventive efficacy of 75.4% at the dose of 2.0 mg/pot, which did not show significant differences compared with those of hymexazol treatments (63.9%). When the dose was 5.0 mg per pot, **I23** achieved a preventive efficacy of 96.5%. The results of the physiological and biochemical analysis, the ultrastructural observation and lipidomics analysis suggested that the mode of action of **I23** might be the disruption of the biological membrane systems of *P. recalcitrans*. In addition, the established CoMFA and CoMSIA models with reasonable statistics in the three-dimensional quantitative structure–activity relationship (3D-QSAR) study revealed the necessity of the C4-carboxyl group and other structural requirements for activity. Overall, the above results would help us to better understand the mode of action and the SAR of these derivatives, and provide crucial information for further design and development of more potent 3,4-dihydroisoquinolin-1(2*H*)-one derivatives as antioomycete agents against *P. recalcitrans*.

Received 8th February 2023
Accepted 27th March 2023

DOI: 10.1039/d3ra00855j

rsc.li/rsc-advances

1. Introduction

Natural products (NPs) have achieved a long tradition as a source of agrochemical active ingredients.[1–3] However, NPs are often perceived as chemically complex molecules and synthetically intractable, have limited availability of resources, or possess undesired substructural elements that impede their suitability for direct application in agricultural settings.[4] More often than not, a prominent exploitation strategy is the simplification of the NP structures and their molecular frameworks to provide a synthetically accessible bioactive scaffold, equivalent or mimic for semisynthetic optimization, ultimately leading to the establishment of the desired compounds for application in crop protection.[4] Correspondingly, such an approach renders synthetic entities of NP mimics that account for 14% of the crop protection product market.[1,4] Particularly, this exploitation strategy could be exemplified by the commercial fungicide florylpicoxamid[5] and insecticide flupyradifurone[6] that have been released on the market recently. Considering these aspects, NP-inspired synthetic scaffolds or mimics can afford feasible and innovative solutions to the aforementioned significant and enduring discovery challenges of crop protection agents.

The fragment of 3,4-dihydroisoquinolin-1(2*H*)-one (**1**) (Fig. 1) is prevalently encountered in numerous NPs with various biological activities.[7,8] Consequently, it has been utilized as a privileged scaffold in the discovery of synthetically accessible drug molecules, such as antitumor,[9–13] antimicrobial,[14–18] antiviral,[19] and antifungal[16] agents. Among the many synthetic approaches explored, the Castagnoli–Cushman reaction (CCR) between homophthalic anhydride and inimes is especially appealing because the reaction not only produces the desired products in high yields, but also offers a remarkably facile and often diastereoselective entry to derivatives of this scaffold that are 2,3-disubstituted and occur a carboxylic acid function at the C4 site.[20,21] By simply drawing from pertinent pools of substrates, this robust, streamlined, straightforward, and flexible approach could enable independent change of substituents around the core scaffold in question, generating diverse chemical libraries for use in the screening of valuable molecules. However, as revealed by thorough literature retrieval, the derivatives of

Department of Pharmaceutical Engineering, College of Plant Protection, Shanxi Key Laboratory of Integrated Pest Management in Agriculture, Shanxi Agricultural University, Taiyuan 030031, China. E-mail: fang_august@163.com; Zhang770504@126.com

† Electronic supplementary information (ESI) available. CCDC 2180985. For ESI and crystallographic data in CIF or other electronic format see DOI: https://doi.org/10.1039/d3ra00855j

‡ These authors contributed equally to this work and share the first authorship.

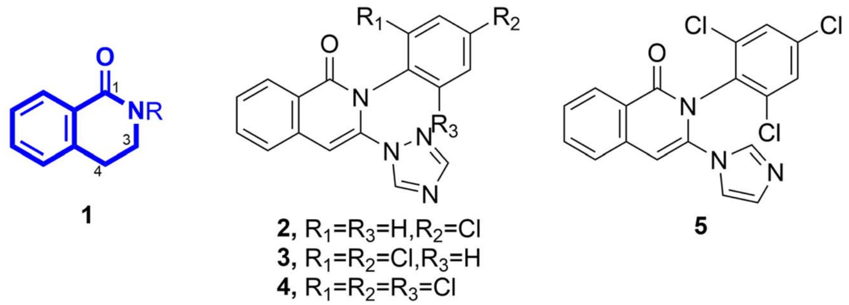

Fig. 1 The structures of 3,4-dihydroisoquinolin-1(2*H*)-one scaffold (**1**) and compounds **2–5** sharing the same carbon skeleton with scaffold **1** with reported *in vivo* bioactivity against some plant pathogens.

scaffold **1** regarding the bioactivity against phytopathogens have received far less attention. Nevertheless, despite the dearth of research, compounds **2–5** (Fig. 1), four isoquinolin-1(2*H*)-one derivatives sharing the same carbon skeleton with scaffold **1**, showed moderate *in vivo* control efficacies against *Blumeria graminis* (DC.) Speer, *Puccinia recondite*, *Botrytis cinerea*, and

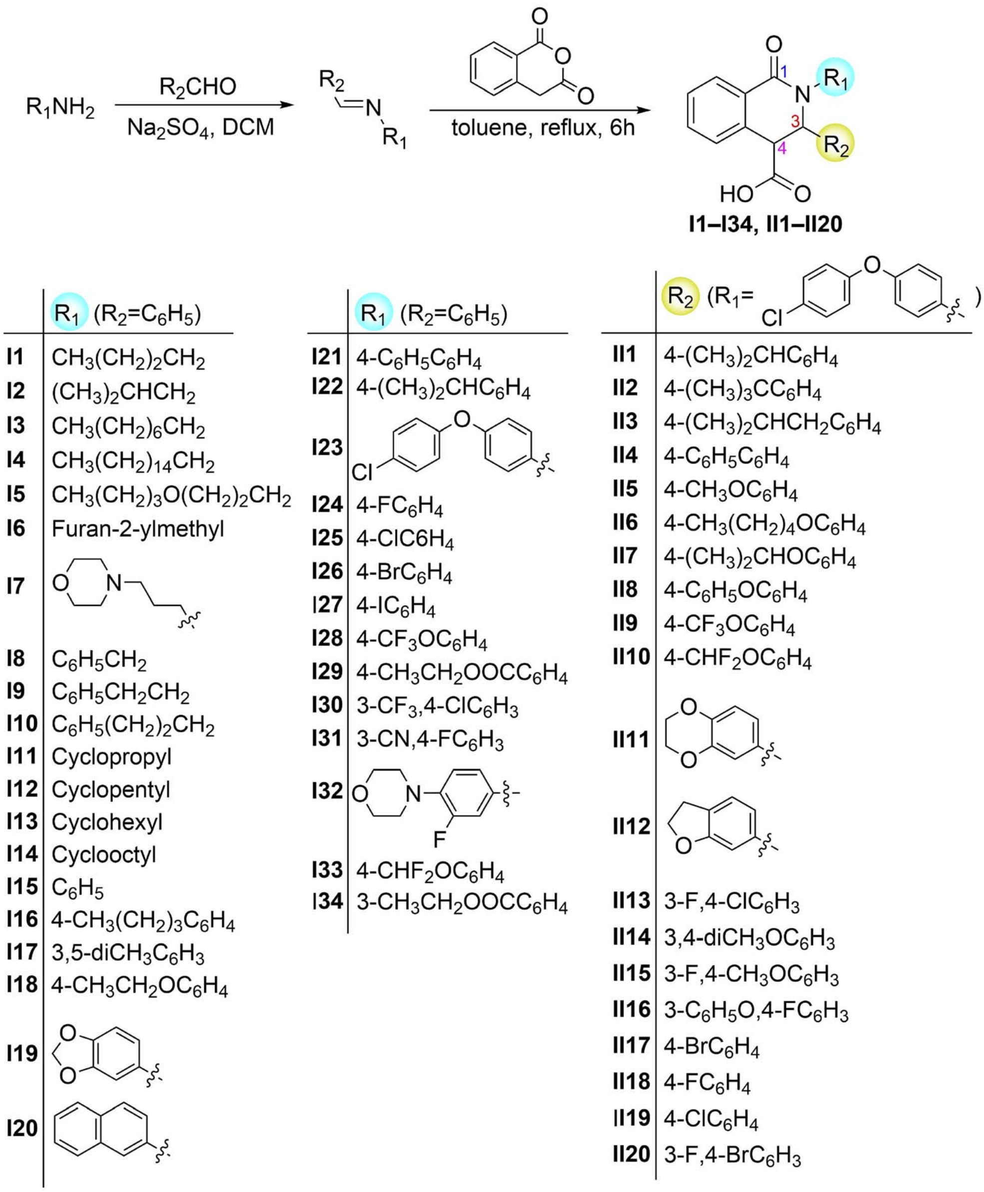

Scheme 1 The synthetic route to the title compounds I1–I34 and II1–II20.

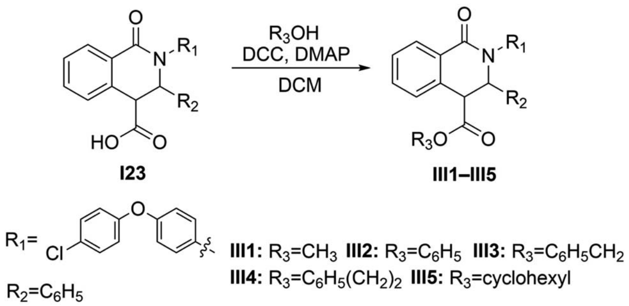

Scheme 2 The synthetic route to the title compounds III1–III5.

Plasmopara viticola,[22] indicating its potential as a starting point for the development of crop protection agents in the plant disease management.

In the present study, we synthesized 59 derivatives of scaffold **1** by employing the CCR and esterification reaction (Scheme 1 and 2), and then we evaluated their antifungal or antioomycete activities. The obtained compounds exhibited high *in vitro* inhibition activity against the phytopathogen *Pythium recalcitrans*, and their antioomycete activity was optimized *via* sequential incorporation of various substituents to the N2, C3, and C4 sites. The three-dimensional quantitative structure–activity relationship (3D-QSAR) was further studied. Finally, the control efficacy of the most potent compound and its antioomycete effects on the physiological and morphological changes of *P. recalcitrans* were investigated as well.

2. Experimental

2.1 General remarks

The analytical grade reagents used were purchased from Shanghai Aladdin Biochemical Technology Co., Ltd. (China). Dichloromethane (DCM) and toluene, the two reaction solvents, were newly distilled in the reactions before drying under reflux over calcium hydride and sodium wires, respectively. The other starting materials, unless otherwise stated, were utilized without additional purification. On a Bruker AV-400 (or 500) instrument, ^{1}H NMR and proton-decoupled ^{13}C NMR spectra were recorded using $CDCl_3$ or DMSO-d_6 as the solvent. Chemical shifts (δ) are recorded in ppm, relative to the residual solvent peaks ($CDCl_3$, δ 7.26 for ^{1}H and δ 77.36 for ^{13}C; DMSO-d_6, δ 2.50 for ^{1}H and δ 39.52 for ^{13}C). The coupling constants (J) were shown in Hertz. Data of ^{1}H NMR spectra are presented as follows: chemical shift (multiplicity, coupling constants, and the number of hydrogen). The types of peak splitting are as follows: s (singlet), d (doublet), t (triplet), q (quartet), m (multiplet), and bs (broadening singlet). High-resolution ESI mass experiments were operated on a Waters Xevo G2-XS instrument with a Quadrupole-Orbitrap mass analyzer. The X-ray diffraction dataset was collected on an XtaLAB Synergy-R single crystal X-ray diffractometer (Rigaku Corporation, Japan). Column chromatography was performed using silica gel (200–300 mesh) purchased from Qingdao Haiyang Chemical Co., China. Seven plant pathogens, *Pythium recalcitrans*, *B. cinerea*, *Fusarium oxysporum* f. sp. *niveum*, *Trichothecium roseum*, *Colletotrichum gloeosporioides*, *Alternaria mali*, and *Rhizoctonia solani* were used for the bioassay experiment. These isolates kept on sterile potato dextrose agar (PDA; aqueous extract of 200 g of peeled potato, 20 g of dextrose, and 20 g of agar in 1.0 L of distilled water sterilized in an autoclave at 121 °C for 15 min) plates at 4 °C are stored in Plant Pathology Laboratory, College of Plant Protection, Shanxi Agricultural University and are available from the authors upon request. Sterile potato dextrose broth (PDB; aqueous extract of 200 g of peeled potato and 20 g of dextrose in 1.0 L of distilled water sterilized in an autoclave at 121 °C for 15 min) was used for culture of *P. recalcitrans* mycelia. For the lipidomics experiment, mass spectrometry grade reagents methanol (CH_3OH), acetonitrile (CH_3CN), 2-propanol, and methyl-*tert*-butyl ether (MTBE) were purchased from Thermo Fisher and HPLC-grade formic acid and ammonium formate were purchased from Sigma.

2.2 Synthesis of 3,4-dihydroisoquinolin-1(2*H*)-one derivatives

2.2.1 General procedure for the synthesis of compounds I1–I34 and II1–II20. The routes to synthesize the target compounds **I1–I34** and **II1–II20** are shown in Scheme 1 and 2, following the reported methods.[23,24] To a dry 25 mL round-bottom flask was added anhydrous sodium sulfate (Na_2SO_4) (15.0 mmol), aromatic aldehyde (5.5 mmol), amine (5.0 mmol), and 10 mL of dry DCM successively. The mixture was stirred at room temperature for 24 h. Upon the reaction being completed using TLC for monitoring, the solid was removed by filtration and the residue was evaporated under reduced pressure. The crude product was washed with ethanol several times and concentrated to obtain the intermediate imine **6.** To a solution of homophthalic anhydride (3.0 mmol) in 20 mL dry toluene was added the above-prepared imine (3.0 mmol) in a 25 mL round-bottom flask equipped with a condenser and the mixture was stirred and refluxed for 6 h. The resulting mixture was cooled to room temperature and the precipitation was collected using vacuum filtration. Finally, the target products were obtained by recrystallization from acetonitrile.

2-Butyl-1-oxo-3-phenyl-1,2,3,4-tetrahydroisoquinoline-4-carboxylic acid (**I1**): white powder, yield 508 mg (52.4%), mp 206–208 °C. ^{1}H NMR (400 MHz, DMSO-d_6) δ_H (ppm): 13.15 (s, 1H), 7.93–7.91 (m, 1H), 7.40–7.36 (m, 2H), 7.26–7.17 (m, 4H), 7.07–7.06 (m, 2H), 5.34 (s, 1H), 4.13 (s, 1H), 4.04–3.97 (m, 1H), 2.77–2.70 (m, 1H), 1.54–1.50 (m, 2H), 1.29–1.23 (m, 2H), 0.86 (t, J = 7.2 Hz, 3H). ^{13}C NMR (100 MHz, DMSO-d_6) δ_C (ppm): 172.6, 163.4, 140.0, 134.1, 132.1, 130.0, 129.6, 129.0, 128.2, 127.9, 127.2, 126.5, 61.1, 51.1, 46.0, 30.0, 20.1, 14.3. HRMS (ESI) m/z: $[M + H]^+$, calcd for $C_{20}H_{22}NO_3$: 324.1600, found: 324.1596.

2-Isobutyl-1-oxo-3-phenyl-1,2,3,4-tetrahydroisoquinoline-4-carboxylic acid (**I2**): white powder, yield 553 mg (57%), mp 176–178 °C. ^{1}H NMR (400 MHz, DMSO-d_6) δ_H (ppm): 13.18 (s, 1H), 7.98–7.96 (m, 1H), 7.41–7.38 (m, 2H), 7.27–7.18 (m, 4H), 7.08–7.06 (m, 2H), 5.36 (s, 1H), 4.18 (s, 1H), 3.96–3.91 (m, 1H), 2.49–2.45 (m, 1H), 2.06–1.99 (m, 1H), 0.89 (d, J = 6.4 Hz, 3H), 0.85 (d, J = 6.4 Hz, 3H). ^{13}C NMR (100 MHz, DMSO-d_6) δ_C (ppm): 172.3, 163.6, 139.4, 133.6, 131.7, 129.6, 129.1, 128.6, 127.8, 127.4, 126.9, 126.0, 61.1, 52.8, 50.7, 26.9, 20.3, 20.2. HRMS (ESI) *m/z*: $[M + H]^+$, calcd for $C_{20}H_{22}NO_3$: 324.1600, found: 324.1596.

2-Octyl-1-oxo-3-phenyl-1,2,3,4-tetrahydroisoquinoline-4-carboxylic acid (**I3**): white powder, yield 603 mg (53%), mp 212–214 °C. ^{1}H NMR (400 MHz, DMSO-d_6) δ_H (ppm): 13.04 (s, 1H), 7.92–7.91 (m, 1H), 7.41–7.36 (m, 2H), 7.25–7.16 (m, 4H), 7.07–7.05 (m, 2H), 5.33 (s, 1H), 4.11 (s, 1H), 3.99–3.93 (m, 1H), 2.77–2.72 (m, 1H), 1.54–1.52 (m, 2H), 1.22 (m, 10H), 0.85 (t, J = 5.2 Hz, 3H). ^{13}C NMR (100 MHz, DMSO-d_6) δ_C (ppm): 172.6, 163.4, 140.1, 134.1, 132.1, 130.0, 129.7, 129.0, 128.2, 127.9, 127.2, 126.5, 61.2, 51.2, 46.4, 31.7, 29.3, 29.1, 27.8, 26.9, 22.6, 14.4. HRMS (ESI) *m/z*: $[M + H]^+$, calcd for $C_{24}H_{30}NO_3$: 380.2226, found: 380.2224.

2-Hexadecyl-1-oxo-3-phenyl-1,2,3,4-tetrahydroisoquinoline-4-carboxylic acid (**I4**): white powder, yield 833 mg (56.5%), mp 224–226 °C. ^{1}H NMR (400 MHz, DMSO-d_6) δ_H (ppm): 13.02 (s, 1H), 8.03–8.02 (m, 1H), 7.54–7.48 (m, 2H), 7.44–7.41 (m, 1H), 7.21–7.18 (m, 3H), 7.01–6.99 (m, 2H), 5.09 (d, J = 4.8 Hz, 1H), 4.70 (d, J = 4.4 Hz, 1H), 3.84–3.78 (m, 1H), 2.86–2.81 (m, 1H), 1.53–1.52 (m, 1H), 1.44–1.43 (m, 1H), 1.20 (m, 26H), 0.84 (t, J = 5.2 Hz, 3H). ^{13}C NMR (100 MHz, DMSO-d_6) δ_C (ppm): 170.8, 163.1, 137.9, 133.9, 132.2, 129.6, 128.6, 128.5, 128.3, 128.2, 127.8, 127.7, 61.7, 48.7, 46.2, 31.8, 29.6, 29.5, 29.4, 29.2, 27.8, 26.9, 22.6, 14.4. HRMS (ESI) *m/z*: $[M + H]^+$, calcd for $C_{32}H_{46}NO_3$: 492.3478, found: 492.3484.

2-(3-Butoxypropyl)-1-oxo-3-phenyl-1,2,3,4-tetrahydroisoquinoline-4-carboxylic acid (**I5**): white powder, yield 789 mg (69%), mp 236–238 °C. ^{1}H NMR (400 MHz, DMSO-d_6) δ_H (ppm): 13.06 (s, 1H), 7.94–7.92 (m, 1H), 7.40–7.37 (m, 2H), 7.26–7.18 (m, 4H), 7.07–7.06 (m, 2H), 5.33 (s, 1H), 4.13 (s, 1H), 4.04–4.00 (m, 1H), 3.40–3.33 (m, 4H), 2.84–2.79 (m, 1H), 1.83–1.74 (m, 2H), 1.47–1.44 (m, 2H), 1.32–1.27 (m, 2H), 0.86 (t, J = 6.0 Hz, 3H). ^{13}C NMR (100 MHz, DMSO-d_6) δ_C (ppm): 172.1, 163.0, 139.5, 133.5, 131.7, 129.6, 129.1, 128.6, 127.8, 127.5, 126.8, 126.0, 69.7, 67.6, 60.9, 50.6, 43.6, 31.4, 27.9, 18.9, 13.8. HRMS (ESI) *m/z*: $[M + H]^+$, calcd for $C_{23}H_{28}NO_4$: 382.2018, found: 382.2022.

2-(Furan-2-ylmethyl)-1-oxo-3-phenyl-1,2,3,4-tetrahydroisoquinoline-4-carboxylic acid (**I6**): white powder, yield 781 mg (75%), mp 238–239 °C. ^{1}H NMR (400 MHz, DMSO-d_6) δ_H (ppm): 12.99 (s, 1H), 8.03–8.01 (m, 1H), 7.48 (s, 1H), 7.42–7.40 (m, 2H), 7.21–7.15 (m, 4H), 7.04–7.02 (m, 2H), 6.31 (s, 2H), 5.39 (s, 1H), 5.12 (d, J = 12.4 Hz, 1H), 4.23 (d, J = 12.4 Hz, 1H), 4.14 (s, 1H). ^{13}C NMR (100 MHz, DMSO-d_6) δ_C (ppm): 172.0, 163.0, 150.0, 142.6, 139.0, 133.7, 132.1, 129.6, 128.9, 128.5, 128.0, 127.4, 127.1, 125.9, 110.4, 108.9, 60.7, 50.8, 42.0. HRMS (ESI) *m/z*: $[M + H]^+$, calcd for $C_{21}H_{18}NO_4$: 348.1236, found: 348.1229.

2-(3-Morpholinopropyl)-1-oxo-3-phenyl-1,2,3,4-tetrahydroisoquinoline-4-carboxylic acid (**I7**): white powder, yield 869 mg (73.5%), mp 221–223 °C. ^{1}H NMR (400 MHz, DMSO-d_6) δ_H (ppm): 13.00 (s, 1H), 7.92–7.91 (m, 1H), 7.40–7.34 (m, 2H), 7.26–7.18 (m, 4H), 7.07–7.05 (m, 2H), 5.36 (s, 1H), 4.06 (s, 1H), 4.03–3.98 (m, 1H), 3.57 (t, J = 1.6 Hz, 4H), 2.81–2.76 (m, 1H), 2.40–2.35 (m, 6H), 1.80–1.71 (m, 2H). ^{13}C NMR (100 MHz, DMSO-d_6) δ_C (ppm): 172.3, 163.1, 139.8, 134.1, 131.6, 129.5, 129.1, 128.6, 127.6, 127.4, 126.7, 126.0, 65.9, 61.1, 55.2, 52.9, 51.1, 44.2, 24.1. HRMS (ESI) *m/z*: $[M + H]^+$, calcd for $C_{23}H_{27}N_2O_4$: 395.1971, found: 395.1967.

2-Benzyl-1-oxo-3-phenyl-1,2,3,4-tetrahydroisoquinoline-4-carboxylic acid (**I8**): white powder, yield 772 mg (72%), mp 171–173 °C. ^{1}H NMR (400 MHz, DMSO-d_6) δ_H (ppm): 13.03 (s, 1H), 8.07–8.06 (m, 1H), 7.44–7.42 (m, 2H), 7.30–7.19 (m, 9H), 7.08–7.07 (m, 2H), 5.35 (s, 1H), 5.32 (d, J = 12.0 Hz, 1H), 4.14 (s, 1H), 3.91 (d, J = 12.0 Hz, 1H). ^{13}C NMR (100 MHz, DMSO-d_6) δ_C (ppm): 172.1, 163.5, 139.2, 137.2, 133.6, 132.0, 129.6, 129.0, 128.7, 128.2, 128.0, 128.0, 127.6, 127.1, 127.0, 126.1, 61.3, 50.9, 49.4. HRMS (ESI) *m/z*: $[M + H]^+$, calcd for $C_{23}H_{20}NO_3$: 358.1443, found: 358.1433.

1-Oxo-2-phenethyl-3-phenyl-1,2,3,4-tetrahydroisoquinoline-4-carboxylic acid (**I9**): white powder, yield 855 mg (76.8%), mp 168–170 °C. ^{1}H NMR (400 MHz, DMSO-d_6) δ_H (ppm): 13.07 (s, 1H), 7.96–7.94 (m, 1H), 7.43–7.38 (m, 2H), 7.29–7.18 (m, 9H), 7.12–7.10 (m, 2H), 5.54 (s, 1H), 4.19 (s, 1H), 4.18–4.12 (m, 1H), 3.05–2.92 (m, 2H), 2.80–2.74 (m, 1H). ^{13}C NMR (100 MHz, DMSO-d_6) δ_C (ppm): 172.1, 162.8, 139.5, 138.9, 133.7, 131.8, 129.6, 129.1, 128.6, 128.4, 128.2, 127.8, 127.4, 126.8, 126.2, 126.1, 60.8, 50.6, 48.0, 33.6. HRMS (ESI) *m/z*: $[M + H]^+$, calcd for $C_{24}H_{22}NO_3$: 372.1600, found: 372.1589.

1-Oxo-3-phenyl-2-(3-phenylpropyl)-1,2,3,4-tetrahydroisoquinoline-4-carboxylic acid (**I10**): white powder, yield 811 mg (70.2%), mp 164–166 °C. ^{1}H NMR (400 MHz, DMSO-d_6) δ_H (ppm): 13.09 (s, 1H), 7.97–7.95 (m, 1H), 7.42–7.37 (m, 2H), 7.28–7.17 (m, 9H), 7.09–7.07 (m, 2H), 5.39 (s, 1H), 4.16 (s, 1H), 4.12–4.06 (m, 1H), 2.83–2.78 (m, 1H), 2.61–2.56 (m, 2H), 1.88 (t, J = 6.4 Hz, 2H). ^{13}C NMR (100 MHz, DMSO-d_6) δ_C (ppm): 172.2, 163.0, 141.9, 139.5, 133.5, 131.8, 129.6, 129.1, 128.6, 128.3, 127.8, 127.5, 126.8, 126.1, 125.7, 60.6, 50.6, 45.7, 32.7, 29.5. HRMS (ESI) *m/z*: $[M + H]^+$, calcd for $C_{25}H_{24}NO_3$: 386.1756, found: 386.1754.

2-Cyclopropyl-1-oxo-3-phenyl-1,2,3,4-tetrahydroisoquinoline-4-carboxylic acid (**I11**): white powder, yield 733 mg (79.5%), mp 155–157 °C. ^{1}H NMR (400 MHz, DMSO-d_6) δ_H (ppm): 13.01 (s, 1H), 7.94–7.92 (m, 1H), 7.40–7.36 (m, 2H), 7.27–7.21 (m, 3H), 7.19–7.17 (m, 1H), 7.12–7.11 (m, 2H), 5.30 (s, 1H), 4.17 (s, 1H), 2.80–2.77 (m, 1H), 0.92–0.90 (m, 1H), 0.77–0.74 (m, 1H), 0.67–0.56 (m, 2H). ^{13}C NMR (100 MHz, DMSO-d_6) δ_C (ppm): 172.0, 164.6, 139.8, 133.5, 131.9, 129.7, 129.1, 128.6, 127.7, 127.3, 126.8, 125.8, 61.6, 50.7, 29.7, 8.2, 5.3. HRMS (ESI) *m/z*: $[M + H]^+$, calcd for $C_{19}H_{18}NO_3$: 308.1287, found: 308.1283.

2-Cyclopentyl-1-oxo-3-phenyl-1,2,3,4-tetrahydroisoquinoline-4-carboxylic acid (**I12**): white powder, yield 784 mg (78%), mp 172–175 °C. ^{1}H NMR (400 MHz, DMSO-d_6) δ_H (ppm): 13.04 (s, 1H), 7.93–7.91 (m, 1H), 7.37–7.35 (m, 2H), 7.22–7.19 (m, 2H), 7.15–7.14 (m, 2H), 7.09–7.08 (m, 2H), 5.32 (s, 1H), 4.90–4.83 (m, 1H), 4.10 (s, 1H), 1.78–1.74 (m, 2H), 1.66–1.63 (m, 1H), 1.57–1.50 (m, 2H), 1.45–1.37 (m, 2H), 1.27–1.18 (m, 1H). ^{13}C NMR (100 MHz, DMSO-d_6) δ_C (ppm): 171.9, 163.1, 141.0, 133.1, 131.5, 130.1, 129.2, 128.4, 127.7, 127.1, 126.8, 125.9, 57.1, 55.2, 51.3, 28.8, 28.0, 23.3, 22.7. HRMS (ESI) *m/z*: $[M + H]^+$, calcd for $C_{21}H_{22}NO_3$: 336.1600, found: 336.1591.

2-Cyclohexyl-1-oxo-3-phenyl-1,2,3,4-tetrahydroisoquinoline-4-carboxylic acid (**I13**): white powder, yield 852 mg (81.3%), mp

188–190 °C. ^{1}H NMR (400 MHz, DMSO-d_6) δ_H (ppm): 13.03 (s, 1H), 7.95–7.93 (m, 1H), 7.37–7.36 (m, 2H), 7.20–7.07 (m, 6H), 5.40 (s, 1H), 4.49–4.46 (m, 1H), 4.03 (s, 1H), 1.76–1.74 (m, 1H), 1.66–1.52 (m, 4H), 1.34–1.31 (m, 2H), 1.21–1.16 (m, 1H), 1.08–0.99 (m, 2H). ^{13}C NMR (100 MHz, DMSO-d_6) δ_C (ppm): 171.9, 162.5, 141.3, 133.0, 131.5, 130.3, 129.2, 128.2, 127.8, 127.1, 126.9, 126.1, 56.8, 53.2, 51.7, 30.1, 29.9, 25.5, 25.4, 24.9. HRMS (ESI) *m/z*: [M + H]$^+$, calcd for $C_{22}H_{24}NO_3$: 350.1756, found: 350.1750.

2-Cyclooctyl-1-oxo-3-phenyl-1,2,3,4-tetrahydroisoquinoline-4-carboxylic acid (**I14**): white powder, yield 877 mg (77.5%), mp 185–188 °C. ^{1}H NMR (400 MHz, DMSO-d_6) δ_H (ppm): 13.08 (s, 1H), 7.96–7.94 (m, 1H), 7.38–7.35 (m, 2H), 7.20–7.07 (m, 6H), 5.35 (s, 1H), 3.99 (s, 1H), 1.97–1.93 (m, 1H), 1.71–1.44 (m, 14H). ^{13}C NMR (100 MHz, DMSO-d_6) δ_C (ppm): 172.2, 162.2, 141.3, 133.0, 131.4, 130.5, 129.1, 128.3, 127.8, 127.2, 126.9, 126.2, 58.6, 55.1, 51.8, 31.3, 30.3, 26.1, 26.0, 25.5, 24.8, 24.2. HRMS (ESI) *m/z*: [M + H]$^+$, calcd for $C_{24}H_{28}NO_3$: 378.2069, found: 378.2067.

1-Oxo-2,3-diphenyl-1,2,3,4-tetrahydroisoquinoline-4-carboxylic acid (**I15**): white powder, yield 690 mg (67%), mp 202–203 °C. ^{1}H NMR (400 MHz, DMSO-d_6) δ_H (ppm): 13.03 (s, 1H), 8.09–8.07 (m, 1H), 7.62–7.57 (m, 2H), 7.52–7.48 (m, 1H), 7.33–7.29 (m, 2H), 7.20–7.16 (m, 6H), 7.05–7.03 (m, 2H), 5.50 (d, J = 5.6 Hz, 1H), 4.96 (d, J = 5.6 Hz, 1H). ^{13}C NMR (100 MHz, DMSO-d_6) δ_C (ppm): 170.5, 162.9, 141.7, 137.3, 134.3, 132.3, 129.2, 128.6, 128.2, 128.0, 127.9, 127.8, 127.6, 127.4, 126.6, 64.4, 49.0. HRMS (ESI) *m/z*: [M + H]$^+$, calcd for $C_{22}H_{18}NO_3$: 344.1287, found: 344.1277.

2-(4-Butylphenyl)-1-oxo-3-phenyl-1,2,3,4-tetrahydroisoquinoline-4-carboxylic acid (**I16**): white powder, yield 650 mg (64.3%), mp 186–188 °C. ^{1}H NMR (400 MHz, DMSO-d_6) δ_H (ppm): 13.03 (s, 1H), 8.10–8.08 (m, 1H), 7.62–7.53 (m, 2H), 7.48–7.45 (m, 1H), 7.15–7.04 (m, 9H), 5.46 (d, J = 4.0 Hz, 1H), 4.97 (d, J = 4.0 Hz, 1H), 2.50 (t, J = 6.0 Hz, 2H), 1.51–1.48 (m, 2H), 1.28–1.24 (m, 2H), 0.86 (t, J = 5.6 Hz, 3H). ^{13}C NMR (100 MHz, DMSO-d_6) δ_C (ppm): 170.4, 162.9, 140.7, 139.4, 137.3, 134.1, 132.2, 129.3, 128.4, 128.1, 128.0, 127.8, 127.8, 127.6, 127.1, 64.6, 49.0, 34.4, 33.0, 21.8, 13.8. HRMS (ESI) *m/z*: [M + H]$^+$, calcd for $C_{26}H_{26}NO_3$: 400.1913, found: 400.1903.

2-(3,5-Dimethylphenyl)-1-oxo-3-phenyl-1,2,3,4-tetrahydroisoquinoline-4-carboxylic acid (**I17**): white powder, yield 702 mg (63%), mp 189–191 °C. ^{1}H NMR (400 MHz, DMSO-d_6) δ_H (ppm): 13.09 (s, 1H), 8.12–8.11 (m, 1H), 7.66–7.47 (m, 3H), 7.18–7.17 (m, 3H), 7.06–6.85 (m, 5H), 5.47 (d, J = 4.8 Hz, 1H), 5.02 (d, J = 4.8 Hz, 1H), 2.18 (s, 6H). ^{13}C NMR (100 MHz, DMSO-d_6) δ_C (ppm): 170.5, 162.8, 141.8, 137.8, 137.3, 134.1, 132.3, 129.4, 128.3, 128.2, 128.1, 127.9, 127.9, 127.8, 127.6, 125.1, 64.7, 48.9, 20.8. HRMS (ESI) *m/z*: [M + H]$^+$, calcd for $C_{24}H_{22}NO_3$: 372.1600, found: 372.1589.

2-(4-Ethoxyphenyl)-1-oxo-3-phenyl-1,2,3,4-tetrahydroisoquinoline-4-carboxylic acid (**I18**): white powder, yield 872 mg (75.1%), mp 207–209 °C. ^{1}H NMR (400 MHz, DMSO-d_6) δ_H (ppm): 13.04 (s, 1H), 8.09–8.07 (m, 1H), 7.62–7.55 (m, 2H), 7.50–7.47 (m, 1H), 7.18–7.16 (m, 3H), 7.09–7.03 (m, 2H), 7.03–7.01 (m, 2H), 6.85–6.82 (m, 2H), 5.42 (d, J = 5.6 Hz, 1H), 4.97 (d, J = 5.6 Hz, 1H), 3.96 (q, J = 6.8 Hz, 2H), 1.29 (t, J = 6.8 Hz, 3H). ^{13}C NMR (100 MHz, DMSO-d_6) δ_C (ppm): 170.9, 163.4, 157.4, 137.8, 134.8, 134.7, 132.7, 129.7, 129.0, 128.6, 128.4, 128.4, 128.3, 128.2, 128.0, 114.7, 65.2, 63.6, 49.4, 15.1. HRMS (ESI) *m/z*: [M + H]$^+$, calcd for $C_{24}H_{22}NO_4$: 388.1549, found: 372.1549.

2-(Benzo[*d*][1,3]dioxol-5-yl)-1-oxo-3-phenyl-1,2,3,4-tetrahydroisoquinoline-4-carboxylic acid (**I19**): white powder, yield 779 mg (67.1%), mp 217–219 °C. ^{1}H NMR (400 MHz, DMSO-d_6) δ_H (ppm): 13.03 (s, 1H), 8.09–8.07 (m, 1H), 7.61–7.56 (m, 2H), 7.50–7.47 (m, 1H), 7.19–7.18 (m, 3H), 7.05–7.04 (m, 2H), 6.84–6.78 (m, 2H), 6.63–6.61 (m, 1H), 6.00 (s, 1H), 5.98 (s, 1H), 5.42 (d, J = 4.8 Hz, 1H), 4.95 (d, J = 4.8 Hz, 1H). ^{13}C NMR (100 MHz, DMSO-d_6) δ_C (ppm): 170.5, 163.1, 147.1, 145.8, 137.2, 135.6, 134.3, 132.3, 129.2, 128.2, 128.1, 128.0, 127.8, 127.6, 120.8, 118.1, 108.9, 107.8, 101.5, 64.8, 49.0. HRMS (ESI) *m/z*: [M + H]$^+$, calcd for $C_{23}H_{18}NO_5$: 388.1185, found: 388.1195.

2-(Naphthalen-2-yl)-1-oxo-3-phenyl-1,2,3,4-tetrahydroisoquinoline-4-carboxylic acid (**I20**): white powder, yield 866 mg (73.4%), mp 195–198 °C. ^{1}H NMR (400 MHz, DMSO-d_6) δ_H (ppm): 13.08 (s, 1H), 8.15–8.13 (m, 1H), 7.87–7.79 (m, 4H), 7.66–7.60 (m, 3H), 7.54–7.51 (m, 1H), 7.49–7.47 (m, 2H), 7.39–7.37 (m, 1H), 7.15–7.11 (m, 4H), 5.70 (d, J = 4.8 Hz, 1H), 5.01 (d, J = 4.8 Hz, 1H). ^{13}C NMR (100 MHz, DMSO-d_6) δ_C (ppm): 170.6, 163.2, 139.3, 137.2, 134.4, 132.9, 132.4, 131.4, 129.2, 128.2, 128.0, 128.0, 127.9, 127.9, 127.7, 127.7, 127.5, 126.3, 126.2, 125.5, 64.5, 49.2. HRMS (ESI) *m/z*: [M + H]$^+$, calcd for $C_{26}H_{20}NO_3$: 394.1443, found: 394.1444.

2-([1,1′-Biphenyl]-4-yl)-1-oxo-3-phenyl-1,2,3,4-tetrahydroisoquinoline-4-carboxylic acid (**I21**): white powder, yield 864 mg (68.7%), mp 191–193 °C. ^{1}H NMR (400 MHz, DMSO-d_6) δ_H (ppm): 13.06 (s, 1H), 8.16–8.14 (m, 1H), 7.66–7.58 (m, 7H), 7.51–7.50 (m, 1H), 7.45–7.42 (m, 2H), 7.36–7.32 (m, 3H), 7.20–7.19 (m, 2H), 7.12–7.11 (m, 2H), 5.59 (d, J = 4.4 Hz, 1H), 5.03 (d, J = 4.4 Hz, 1H). ^{13}C NMR (100 MHz, DMSO-d_6) δ_C (ppm): 170.5, 163.0, 141.1, 139.4, 138.3, 137.3, 134.2, 132.4, 129.2, 129.0, 128.3, 128.1, 127.9, 127.8, 127.7, 127.6, 126.9, 126.7, 64.4, 49.1. HRMS (ESI) *m/z*: [M + H]$^+$, calcd for $C_{28}H_{22}NO_3$: 420.1600, found: 420.1602.

2-(4-Isopropylphenyl)-1-oxo-3-phenyl-1,2,3,4-tetrahydroisoquinoline-4-carboxylic acid (**I22**): white powder, yield 811 mg (70.2%), mp 214–216 °C. ^{1}H NMR (400 MHz, DMSO-d_6) δ_H (ppm): 13.18 (s, 1H), 8.02–8.0 (m, 1H), 7.48–7.42 (m, 3H), 7.27–7.22 (m, 8H), 7.18–7.17 (m, 1H), 5.69 (s, 1H), 4.25 (s, 1H), 2.89–2.84 (m, 1H), 1.18 (d, J = 5.2 Hz, 6H). ^{13}C NMR (100 MHz, DMSO-d_6) δ_C (ppm): 172.1, 162.7, 146.7, 140.0, 139.3, 133.7, 132.3, 129.7, 129.2, 128.6, 128.0, 127.4, 127.3, 126.6, 126.2, 64.3, 51.1, 33.0, 23.8, 23.8. HRMS (ESI) *m/z*: [M + H]$^+$, calcd for $C_{25}H_{24}NO_3$: 386.1756, found: 386.1754.

2-(4-(4-Chlorophenoxy)phenyl)-1-oxo-3-phenyl-1,2,3,4-tetrahydroisoquinoline-4-carboxylic acid (**I23**): white powder, yield 1.17 g (83%), mp 236–238 °C. ^{1}H NMR (400 MHz, DMSO-d_6) δ_H (ppm): 13.01 (s, 1H), 8.09–8.07 (m, 1H), 7.61–7.58 (m, 3H), 7.51–7.48 (m, 1H), 7.43–7.41 (m, 2H), 7.21–7.19 (m, 4H), 7.06–7.05 (m, 2H), 6.99–6.95 (m, 4H), 5.51 (d, J = 4.8 Hz, 1H), 4.93 (d, J = 4.8 Hz, 1H). ^{13}C NMR (100 MHz, DMSO-d_6) δ_C (ppm): 170.5, 163.0, 155.5, 154.4, 137.3, 137.2, 134.3, 132.3, 129.9, 129.1, 128.2, 128.0, 128.0, 127.8, 127.8, 127.6, 127.3, 120.3, 118.7, 64.4, 49.0. HRMS (ESI) m/z: $[M + H]^+$, calcd for $C_{28}H_{21}ClNO_4$: 470.1159, found: 470.1147.

2-(4-Fluorophenyl)-1-oxo-3-phenyl-1,2,3,4-tetrahydroisoquinoline-4-carboxylic acid (**I24**): white powder, yield 821 mg (75.8%), mp 193–195 °C. ^1H NMR (400 MHz, DMSO-d_6) δ_H (ppm): 12.97 (s, 1H), 8.10–8.09 (m, 1H), 7.62–7.57 (m, 2H), 7.52–7.49 (m, 1H), 7.24–7.21 (m, 2H), 7.19–7.18 (m, 3H), 7.15–7.11 (m, 2H), 7.07–7.05 (m, 2H), 5.51 (d, J = 4.8 Hz, 1H), 4.93 (d, J = 4.8 Hz, 1H). ^{13}C NMR (100 MHz, DMSO-d_6) δ_C (ppm): 170.4, 163.1, 160.2 (d, $^1J_{C-F}$ = 245.5 Hz), 137.8 (d, $^4J_{C-F}$ = 2.5 Hz), 137.1, 134.4, 132.3, 129.5 (d, $^3J_{C-F}$ = 8.8 Hz), 129.0, 128.1, 128.0, 128.0, 127.8, 127.7, 127.6, 115.3 (d, $^2J_{C-F}$ = 23.0 Hz), 64.4, 49.1. HRMS (ESI) m/z: $[M + H]^+$, calcd for $C_{22}H_{17}FNO_3$: 362.1192, found: 362.1189.

2-(4-Chlorophenyl)-1-oxo-3-phenyl-1,2,3,4-tetrahydroisoquinoline-4-carboxylic acid (**I25**): white powder, yield 752 mg (66.4%), mp 200–201 °C. ^1H NMR (400 MHz, DMSO-d_6) δ_H (ppm): 13.03 (s, 1H), 8.08–8.06 (m, 1H), 7.60–7.59 (m, 2H), 7.52–7.48 (m, 2H), 7.38–7.35 (m, 2H), 7.23–7.18 (m, 4H), 7.06–7.04 (m, 2H), 5.54 (d, J = 5.6 Hz, 1H), 4.88 (d, J = 5.6 Hz, 1H). ^{13}C NMR (100 MHz, DMSO-d_6) δ_C (ppm): 170.5, 163.1, 140.4, 137.1, 134.5, 132.5, 130.8, 129.3, 128.9, 128.6, 128.2, 128.1, 128.0, 127.9, 127.8, 127.7, 64.1, 49.1. HRMS (ESI) m/z: $[M + H]^+$ calcd for $C_{22}H_{17}ClNO_3$: 378.0897, found: 378.0888.

2-(4-Bromophenyl)-1-oxo-3-phenyl-1,2,3,4-tetrahydroisoquinoline-4-carboxylic acid (**I26**): white powder, yield 920 mg (72.7%), mp 211–213 °C. ^1H NMR (400 MHz, DMSO-d_6) δ_H (ppm): 12.99 (s, 1H), 8.09–8.08 (m, 1H), 7.60–7.49 (m, 4H), 7.19–7.15 (m, 6H), 7.07–7.05 (m, 2H), 5.55 (d, J = 4.8 Hz, 1H), 4.89 (d, J = 4.8 Hz, 1H). ^{13}C NMR (100 MHz, DMSO-d_6) δ_C (ppm): 170.4, 163.0, 140.8, 137.0, 134.5, 132.5, 131.5, 129.6, 128.9, 128.0, 127.9, 127.9, 127.7, 127.7, 119.2, 64.0, 49.1. HRMS (ESI) m/z: $[M + H]^+$, calcd for $C_{22}H_{17}BrNO_3$: 422.0392, found: 422.0387.

2-(4-Iodophenyl)-1-oxo-3-phenyl-1,2,3,4-tetrahydroisoquinoline-4-carboxylic acid (**I27**): white powder, yield 1.13 g (80.3%), mp 208–210 °C. ^1H NMR (400 MHz, DMSO-d_6) δ_H (ppm): 12.99 (s, 1H), 8.08–8.07 (m, 1H), 7.66–7.59 (m, 4H), 7.51–7.48 (m, 1H), 7.18–7.17 (m, 3H), 7.05–7.01 (m, 4H), 5.53 (d, J = 4.4 Hz, 1H), 4.89 (d, J = 4.4 Hz, 1H). ^{13}C NMR (100 MHz, DMSO-d_6) δ_C (ppm): 170.9, 163.4, 141.8, 137.9, 137.5, 134.9, 133.0, 130.3, 129.4, 128.7, 128.6, 128.4, 128.3, 128.2, 125.8, 92.6, 64.5, 49.6. HRMS (ESI) m/z: $[M + H]^+$, calcd for $C_{22}H_{17}INO_3$: 470.0253, found: 470.0246.

1-Oxo-3-phenyl-2-(4-(trifluoromethoxy)phenyl)-1,2,3,4-tetrahydroisoquinoline-4-carboxylic acid (**I28**): white powder, yield 956 mg (74.6%), mp 211–213 °C. ^1H NMR (400 MHz, DMSO-d_6) δ_H (ppm): 13.03 (s, 1H), 8.10 (m, 1H), 7.61–7.60 (m, 2H), 7.52–7.49 (m, 1H), 7.35–7.30 (m, 4H), 7.19–7.18 (m, 3H), 7.09–7.07 (m, 2H), 5.58 (d, J = 4.4 Hz, 1H), 4.93 (d, J = 4.4 Hz, 1H). ^{13}C NMR (100 MHz, DMSO-d_6) δ_C (ppm): 170.5, 163.1, 146.3, 140.6, 137.0, 134.5, 132.5, 129.3, 128.9, 128.2, 128.1, 128.0, 127.9, 127.8, 127.7, 121.1 (q, $^1J_{C-F}$ = 256.2 Hz), 64.2, 49.2. HRMS (ESI) m/z: $[M + H]^+$, calcd for $C_{23}H_{17}F_3NO_4$: 428.1110, found: 428.1100.

2-(4-(Ethoxycarbonyl)phenyl)-1-oxo-3-phenyl-1,2,3,4-tetrahydroisoquinoline-4-carboxylic acid (**I29**): white powder, yield 869 mg (69.8%), mp 187–189 °C. ^1H NMR (400 MHz, DMSO-d_6) δ_H (ppm): 13.03 (s, 1H), 8.11–8.10 (m, 1H), 7.89–7.87 (m, 2H), 7.61–7.60 (m, 2H), 7.53–7.50 (m, 1H), 7.39–7.37 (m, 2H), 7.18–7.17 (m, 3H), 7.10–7.08 (m, 2H), 5.67 (d, J = 4.4 Hz, 1H), 4.87 (d, J = 4.4 Hz, 1H), 4.28 (q, J = 5.6 Hz, 2H), 1.28 (t, J = 5.6 Hz, 3H). ^{13}C NMR (100 MHz, DMSO-d_6) δ_C (ppm): 170.5, 165.2, 163.1, 145.7, 137.0, 134.5, 132.6, 129.4, 128.9, 128.2, 128.0, 128.0, 127.9, 127.8, 127.7, 127.5, 127.4, 63.8, 60.7, 49.3, 14.1. HRMS (ESI) m/z: $[M + H]^+$, calcd for $C_{25}H_{22}NO_5$: 416.1498, found: 416.1496.

2-(4-Chloro-3-(trifluoromethyl)phenyl)-1-oxo-3-phenyl-1,2,3,4-tetrahydroisoqui-noline-4-carboxylic acid (**I30**): white powder, yield 1.01 g (76.1%), mp 221–223 °C. ^1H NMR (400 MHz, DMSO-d_6) δ_H (ppm): 13.01 (s, 1H), 8.10–8.08 (m, 1H), 7.74–7.73 (m, 1H), 7.65–7.58 (m, 3H), 7.53–7.50 (m, 1H), 7.46–7.44 (m, 1H), 7.21–7.19 (m, 3H), 7.11–7.09 (m, 2H), 5.69 (d, J = 4.4 Hz, 1H), 4.86 (d, J = 4.4 Hz, 1H). ^{13}C NMR (100 MHz, DMSO-d_6) δ_C (ppm): 170.6, 163.4, 140.6, 136.8, 134.8, 133.1, 132.8, 131.8, 128.6, 128.1, 128.0, 127.9, 127.8, 127.0, 126.6 (q, $^2J_{C-F}$ = 31.4 Hz), 122.5 (q, $^1J_{C-F}$ = 273.2 Hz), 63.7, 49.2. HRMS (ESI) m/z: $[M + H]^+$, calcd for $C_{23}H_{16}ClF_3NO_3$: 446.0771, found: 446.0760.

2-(3-Cyano-4-fluorophenyl)-1-oxo-3-phenyl-1,2,3,4-tetrahydroisoquinoline-4-carboxylic acid (**I31**): white powder, yield 759 mg (65.5%), mp 230–233 °C. ^1H NMR (400 MHz, DMSO-d_6) δ_H (ppm): 13.03 (s, 1H), 8.10–8.09 (m, 1H), 7.87–7.85 (m, 1H), 7.62–7.56 (m, 3H), 7.53–7.50 (m, 1H), 7.46–7.42 (m, 1H), 7.21–7.19 (m, 3H), 7.12–7.10 (m, 2H), 5.67 (d, J = 4.4 Hz, 1H), 4.84 (d, J = 4.4 Hz, 1H). ^{13}C NMR (100 MHz, DMSO-d_6) δ_C (ppm): 170.6, 163.4, 160.4 (d, $^1J_{C-F}$ = 255.2 Hz), 138.2 (d, $^4J_{C-F}$ = 3.1 Hz), 136.6, 135.7 (d, $^3J_{C-F}$ = 9.0 Hz), 134.8, 132.8, 128.5, 128.3, 128.2, 128.1, 127.9, 127.8, 116.7 (d, $^2J_{C-F}$ = 20.5 Hz), 113.5, 100.2 (d, $^3J_{C-F}$ = 16.3 Hz), 63.8, 49.3. HRMS (ESI) m/z: $[M + H]^+$, calcd for $C_{23}H_{16}FN_2O_3$: 387.1145, found: 387.1134.

2-(3-Fluoro-4-morpholinophenyl)-1-oxo-3-phenyl-1,2,3,4-tetrahydroisoquino-line-4-carboxylic acid (**I32**): white powder, yield 843 mg (63%), mp 239–241 °C. ^1H NMR (400 MHz, DMSO-d_6) δ_H (ppm): 13.05 (s, 1H), 8.11–8.10 (m, 1H), 7.63–7.56 (m, 2H), 7.50–7.47 (m, 1H), 7.20–7.18 (m, 3H), 7.10–7.06 (m, 3H), 6.94–6.92 (m, 2H), 5.50 (d, J = 4.4 Hz, 1H), 4.97 (d, J = 4.4 Hz, 1H), 3.71 (t, J = 3.6 Hz, 4H), 2.96 (t, J = 3.6 Hz, 4H). ^{13}C NMR (100 MHz, DMSO-d_6) δ_C (ppm): 170.4, 163.0, 154.0 (d, $^1J_{C-F}$ = 244.7 Hz), 138.2 (d, $^3J_{C-F}$ = 8.3 Hz), 137.2, 135.8 (d, $^3J_{C-F}$ = 9.7 Hz), 134.2, 132.4, 129.1, 128.2, 128.1, 127.9, 127.6, 123.6 (d, $^4J_{C-F}$ = 2.7 Hz), 118.4 (d, $^4J_{C-F}$ = 3.7 Hz), 115.5 (d, $^2J_{C-F}$ = 22.2 Hz), 66.2, 64.4, 50.4, 49.0. HRMS (ESI) m/z: $[M + H]^+$, calcd for $C_{26}H_{24}FN_2O_4$: 447.1720, found: 447.1711.

2-(4-(Difluoromethoxy)phenyl)-1-oxo-3-phenyl-1,2,3,4-tetrahydroisoquinoline-4-carboxylic acid (**I33**): white powder, yield 859 mg (70%), mp 205–208 °C. ^1H NMR (400 MHz, DMSO-d_6) δ_H (ppm): 13.01 (s, 1H), 8.10–8.09 (m, 1H), 7.62–7.59 (m, 2H), 7.52–7.49 (m, 1H), 7.27–7.25 (m, 5H), 7.21–7.06 (m, 5H), 5.52 (d, J = 4.4 Hz, 1H), 4.95 (d, J = 4.4 Hz, 1H). ^{13}C NMR (100 MHz, DMSO-d_6) δ_C (ppm): 170.5, 163.1, 149.1, 138.5, 137.1, 134.4, 132.4, 129.1, 129.0, 128.2, 128.1, 127.9, 127.9, 127.8, 127.7, 118.8, 116.3 (t, $^1J_{C-F}$ = 257.2 Hz), 64.4, 49.0. HRMS (ESI) m/z: $[M + H]^+$, calcd for $C_{23}H_{18}F_2NO_4$: 410.1204, found: 410.1192.

2-(3-(Ethoxycarbonyl)phenyl)-1-oxo-3-phenyl-1,2,3,4-tetrahydroisoquinoline-4-carboxylic acid (**I34**): white powder, yield 908 mg (72.9%), mp 196–198 °C. ^{1}H NMR (400 MHz, DMSO-d_6) δ_H (ppm): 13.03 (s, 1H), 8.11–8.09 (m, 1H), 7.84–7.77 (m, 2H), 7.61–7.60 (m, 2H), 7.53–7.50 (m, 1H), 7.44–7.43 (m, 2H), 7.19–7.18 (m, 3H), 7.08–7.06 (m, 2H), 5.60 (d, J = 4.4 Hz, 1H), 4.96 (d, J = 4.4 Hz, 1H), 4.28 (q, J = 5.6 Hz, 2H), 1.28 (t, J = 5.6 Hz, 3H). ^{13}C NMR (100 MHz, DMSO-d_6) δ_C (ppm): 170.5, 165.2, 163.1, 137.1, 134.5, 132.5, 132.1, 130.3, 129.0, 128.9, 128.3, 128.2, 128.1, 128.0, 127.9, 127.8, 127.7, 127.2, 64.1, 60.9, 49.1, 14.1. HRMS (ESI) m/z: [M + H]$^+$, calcd for $C_{25}H_{22}NO_5$: 416.1498, found: 416.1496.

2-(4-(4-Chlorophenoxy)phenyl)-3-(4-isopropylphenyl)-1-oxo-1,2,3,4-tetrahydro-isoquinoline-4-carboxylic acid (**II1**): white powder, yield 1.15 g (75.3%), mp 225–227 °C. ^{1}H NMR (400 MHz, DMSO-d_6) δ_H (ppm): 13.00 (s, 1H), 8.09–8.08 (m, 1H), 7.64–7.62 (m, 1H), 7.59–7.47 (m, 2H), 7.42–7.21 (m, 4H), 7.06–7.05 (m, 2H), 7.00–6.96 (m, 6H), 5.46 (d, J = 4.4 Hz, 1H), 4.96 (d, J = 4.4 Hz, 1H), 2.80–2.75 (m, 1H), 1.11 (d, J = 5.2 Hz, 6H). ^{13}C NMR (100 MHz, DMSO-d_6) δ_C (ppm): 170.4, 162.9, 155.5, 154.4, 147.9, 137.4, 134.4, 134.3, 132.3, 129.9, 129.2, 129.0, 127.8, 127.5, 127.3, 126.1, 120.2, 118.8, 64.3, 48.9, 32.8, 23.6. HRMS (ESI) m/z: [M + H]$^+$, calcd for $C_{31}H_{27}ClNO_4$: 512.1629, found: 512.1626.

3-(4-(*tert*-Butyl)phenyl)-2-(4-(4-chlorophenoxy)phenyl)-1-oxo-1,2,3,4-tetrahydroisoquinoline-4-carboxylic acid (**II2**): white powder, yield 1.14 g (72.7%), mp. 219–221 °C ^{1}H NMR (400 MHz, DMSO-d_6) δ_H (ppm): 13.04 (s, 1H), 8.11–8.09 (m, 1H), 7.65–7.64 (m, 1H), 7.59–7.56 (m, 1H), 7.50–7.47 (m, 1H), 7.41–7.39 (m, 2H), 7.24–7.19 (m, 4H), 6.99–6.95 (m, 6H), 5.47 (d, J = 4.4 Hz, 1H), 4.98 (d, J = 4.4 Hz, 1H), 1.18 (s, 9H). ^{13}C NMR (100 MHz, DMSO-d_6) δ_C (ppm): 170.4, 162.9, 155.5, 154.4, 150.3, 137.5, 134.3, 134.1, 132.3, 129.9, 129.2, 128.9, 127.9, 127.6, 127.5, 127.4, 125.0, 120.3, 118.7, 118.0, 64.3, 48.8, 34.2, 31.0, 31.0. HRMS (ESI) m/z: [M + H]$^+$, calcd for $C_{32}H_{29}ClNO_4$: 526.1785, found: 526.1786.

2-(4-(4-Chlorophenoxy)phenyl)-3-(4-isobutylphenyl)-1-oxo-1,2,3,4-tetrahydroisoquinoline-4-carboxylic acid (**II3**): white powder, yield 1.09 g (69.1%), mp 234–236 °C. ^{1}H NMR (400 MHz, DMSO-d_6) δ_H (ppm): 12.99 (s, 1H), 8.10–8.09 (m, 1H), 7.62–7.56 (m, 2H), 7.50–7.47 (m, 1H), 7.41–7.19 (m, 4H), 6.98–6.93 (m, 8H), 5.48 (d, J = 4.0 Hz, 1H), 4.90 (d, J = 4.0 Hz, 1H), 2.33 (d, J = 5.6 Hz, 2H), 1.76–1.70 (m, 1H), 0.77 (d, J = 5.2 Hz, 6H). ^{13}C NMR (100 MHz, DMSO-d_6) δ_C (ppm): 170.5, 163.0, 155.5, 154.4, 140.9, 137.4, 134.5, 134.5, 132.3, 129.9, 129.1, 128.7, 127.8, 127.8, 127.6, 127.3, 120.2, 118.7, 64.3, 49.1, 44.1, 29.4, 22.1, 22.0. HRMS (ESI) m/z: [M + H]$^+$, calcd for $C_{32}H_{29}ClNO_4$: 526.1785, found: 526.1796.

3-([1,1′-Biphenyl]-4-yl)-2-(4-(4-chlorophenoxy)phenyl)-1-oxo-1,2,3,4-tetrahydroisoquinoline-4-carboxylic acid (**II4**): white powder, yield 1.15 g (70.7%), mp 241–243 °C. ^{1}H NMR (400 MHz, DMSO-d_6) δ_H (ppm): 13.07 (s, 1H), 8.12–8.10 (m, 1H), 7.64–7.59 (m, 4H), 7.52–7.50 (m, 2H), 7.43–7.33 (m, 4H), 7.26–6.96 (m, 10H), 5.57 (d, J = 4.0 Hz, 1H), 4.98 (d, J = 4.0 Hz, 1H). ^{13}C NMR (100 MHz, DMSO-d_6) δ_C (ppm): 170.5, 163.0, 155.5, 154.4, 139.5, 139.1, 137.4, 136.4, 134.4, 132.4, 129.9, 129.1, 128.9, 128.6, 127.9, 127.8, 127.7, 127.6, 127.3, 126.9, 126.5, 126.3, 120.2, 118.8, 64.2, 49.0. HRMS (ESI) m/z: [M + H]$^+$ calcd for $C_{34}H_{25}ClNO_4$: 546.1472, found: 546.1467.

2-(4-(4-Chlorophenoxy)phenyl)-3-(4-methoxyphenyl)-1-oxo-1,2,3,4-tetrahydroisoquinoline-4-carboxylic acid (**II5**): white powder, yield 1.25 g (83.7%), mp 228–230 °C. ^{1}H NMR (400 MHz, DMSO-d_6) δ_H (ppm): 12.93 (s, 1H), 8.09–8.07 (m, 1H), 7.63–7.57 (m, 2H), 7.50–7.48 (m, 1H), 7.43–7.19 (m, 4H), 7.00–6.73 (m, 8H), 5.44 (d, J = 4.4 Hz, 1H), 4.90 (d, J = 4.4 Hz, 1H), 3.66 (s, 3H). ^{13}C NMR (100 MHz, DMSO-d_6) δ_C (ppm): 170.5, 162.9, 158.8, 155.5, 154.4, 137.4, 134.4, 132.3, 129.9, 129.1, 129.0, 127.8, 127.8, 127.6, 127.3, 120.3, 118.8, 113.5, 64.0, 54.9, 49.1. HRMS (ESI) m/z: [M + H]$^+$, calcd for $C_{29}H_{23}ClNO_5$: 500.1265, found: 500.1265.

2-(4-(4-Chlorophenoxy)phenyl)-1-oxo-3-(4-(pentyloxy)phenyl)-1,2,3,4-tetrahydroisoquinoline-4-carboxylic acid (**II6**): white powder, yield 1.31 g (79%), mp 244–246 °C. ^{1}H NMR (400 MHz, DMSO-d_6) δ_H (ppm): 12.97 (s, 1H), 8.08–8.07 (m, 1H), 7.63–7.56 (m, 2H), 7.50–7.47 (m, 1H), 7.42–7.19 (m, 4H), 6.99–6.71 (m, 8H), 5.44 (d, J = 4.4 Hz, 1H), 4.88 (d, J = 4.4 Hz, 1H), 3.84 (t, J = 5.2 Hz, 2H), 1.67–1.62 (m, 2H), 1.36–1.28 (m, 4H), 0.86 (t, J = 5.6 Hz, 3H). ^{13}C NMR (100 MHz, DMSO-d_6) δ_C (ppm): 170.5, 162.9, 158.3, 155.6, 154.3, 137.4, 134.4, 132.2, 129.9, 129.8, 129.1, 128.8, 127.8, 127.8, 127.5, 127.2, 118.8, 113.9, 67.2, 63.9, 49.1, 28.3, 27.7, 21.8, 13.8. HRMS (ESI) m/z: [M + H]$^+$, calcd for $C_{33}H_{31}ClNO_5$: 556.1891, found: 556.1890.

2-(4-(4-Chlorophenoxy)phenyl)-3-(4-isopropoxyphenyl)-1-oxo-1,2,3,4-tetrahydroisoquinoline-4-carboxylic acid (**II7**): white powder, yield 1.14 g (72.4%), mp 238–240 °C. ^{1}H NMR (400 MHz, DMSO-d_6) δ_H (ppm): 12.93 (s, 1H), 8.08–8.06 (m, 1H), 7.62–7.57 (m, 2H), 7.50–7.40 (m, 3H), 7.20–6.69 (m, 10H), 5.42 (d, J = 4.4 Hz, 1H), 4.87 (d, J = 4.4 Hz, 1H), 4.51–4.47 (m, 1H), 1.18 (d, J = 4.8 Hz, 6H). ^{13}C NMR (100 MHz, DMSO-d_6) δ_C (ppm): 170.5, 162.9, 157.1, 155.6, 154.3, 137.4, 134.5, 132.2, 129.8, 129.2, 129.1, 128.7, 127.8, 127.6, 127.3, 120.2, 118.8, 114.9, 69.0, 64.0, 49.1, 21.8, 21.7. HRMS (ESI) m/z: [M + H]$^+$, calcd for $C_{31}H_{27}ClNO_5$, 528.1578, found: 528.1577.

2-(4-(4-Chlorophenoxy)phenyl)-1-oxo-3-(4-phenoxyphenyl)-1,2,3,4-tetrahydroisoquinoline-4-carboxylic acid (**II8**): white powder, yield 1.29 g (76.7%), mp 246–248 °C. ^{1}H NMR (400 MHz, DMSO-d_6) δ_H (ppm): 13.03 (s, 1H), 8.10–8.08 (m, 1H), 7.63–7.59 (m, 2H), 7.51–7.49 (m, 1H), 7.42–7.10 (m, 6H), 7.07–6.97 (m, 7H), 6.91–6.80 (m, 4H), 5.52 (d, J = 4.4 Hz, 1H), 4.93 (d, J = 4.4 Hz, 1H). ^{13}C NMR (100 MHz, DMSO-d_6) δ_C (ppm): 170.6, 163.0, 156.3, 156.2, 155.5, 154.5, 137.3, 134.4, 132.4, 132.1, 130.0, 129.9, 129.7, 129.3, 129.1, 127.9, 127.7, 127.4, 123.7, 120.3, 118.7, 118.0, 63.9, 49.1. HRMS (ESI) m/z: [M + H]$^+$, calcd for $C_{34}H_{25}ClNO_5$: 562.1421, found: 562.1416.

2-(4-(4-Chlorophenoxy)phenyl)-1-oxo-3-(4-(trifluoromethoxy)phenyl)-1,2,3,4-tetrahydroisoquinoline-4-carboxylic acid (**II9**): white powder, yield 1.31 g (79.4%), mp 249–251 °C. ^{1}H NMR (400 MHz, DMSO-d_6) δ_H (ppm): 12.99 (s, 1H), 8.10–8.08 (m, 1H), 7.62–7.59 (m, 2H), 7.42–7.39 (m, 3H), 7.22–7.19 (m, 6H), 6.99–6.96 (m, 4H), 5.61 (d, J = 4.4 Hz, 1H), 4.93 (d, J = 4.4 Hz, 1H). ^{13}C NMR (100 MHz, DMSO-d_6) δ_C (ppm): 170.5, 163.0, 155.5, 154.5, 137.0, 136.6, 134.2, 132.5, 130.0, 129.9, 129.3, 128.9, 128.3, 128.3, 128.0, 127.8, 127.4, 121.0, 120.5, 120.3, 118.8, 63.5, 49.0.

HRMS (ESI) m/z: $[M + H]^+$, calcd for $C_{29}H_{20}ClF_3NO_5$: 554.0982, found: 554.0982.

2-(4-(4-Chlorophenoxy)phenyl)-3-(4-(difluoromethoxy)phenyl)-1-oxo-1,2,3,4-tetrahydroisoquinoline-4-carboxylic acid (**II10**): white powder, yield 1.19 g (74.2%), mp 248–250 °C. ^1H NMR (400 MHz, DMSO-d_6) δ_H (ppm): 13.04 (s, 1H), 8.09–8.08 (m, 1H), 7.60–7.50 (m, 3H), 7.43–7.41 (m, 2H), 7.23–7.09 (m, 2H), 7.01–6.97 (m, 9H), 5.54 (d, J = 4.4 Hz, 1H), 4.93 (d, J = 4.4 Hz, 1H). ^{13}C NMR (100 MHz, DMSO-d_6) δ_C (ppm): 170.5, 163.0, 155.5, 154.5, 150.5, 137.2, 134.2, 133.9, 132.4, 129.9, 129.7, 129.2, 129.0, 127.9, 127.8, 127.7, 127.4, 120.3, 118.8, 117.1 (t, $^1J_{C-F}$ = 260.1 Hz), 63.7, 49.0. HRMS (ESI) m/z: $[M + H]^+$, calcd for $C_{29}H_{21}ClF_2NO_5$: 536.1076, found: 536.1077.

2-(4-(4-Chlorophenoxy)phenyl)-3-(2,3-dihydrobenzo[*b*][1,4]dioxin-6-yl)-1-oxo-1,2,3,4-tetrahydroisoquinoline-4-carboxylic acid (**II11**): white powder, yield 1.11 g (69.9%), mp 251–253C. ^1H NMR (400 MHz, DMSO-d_6) δ_H (ppm): 13.03 (s, 1H), 8.06–8.04 (m, 1H), 7.64–7.62 (m, 1H), 7.60–7.57 (m, 1H), 7.50–7.43 (m, 3H), 7.21–7.20 (m, 2H), 7.02–6.99 (m, 4H), 6.67–6.48 (m, 3H), 5.36 (d, J = 3.6 Hz, 1H), 4.91 (d, J = 3.6 Hz, 1H), 4.14 (s, 2H), 4.13 (s, 2H). ^{13}C NMR (100 MHz, DMSO-d_6) δ_C (ppm): 170.5, 162.9, 155.6, 154.4, 143.1, 142.7, 137.4, 134.4, 132.3, 130.1, 129.9, 129.1, 129.0, 127.9, 127.8, 127.6, 127.3, 120.9, 120.3, 118.8, 116.7, 116.5, 63.9, 63.9, 48.9. HRMS (ESI) m/z: $[M + H]^+$, calcd for $C_{30}H_{23}ClNO_6$: 528.1214, found: 528.1211.

2-(4-(4-Chlorophenoxy)phenyl)-3-(2,3-dihydrobenzofuran-5-yl)-1-oxo-1,2,3,4-tetrahydroisoquinoline-4-carboxylic acid (**II12**): white powder, yield 1.05 g (68.3%), mp 252–254 °C. ^1H NMR (400 MHz, DMSO-d_6) δ_H (ppm): 13.04 (s, 1H), 8.01–8.00 (m, 1H), 7.49–7.46 (m, 1H), 7.44–7.35 (m, 2H), 7.32–7.04 (m, 3H), 7.07–7.03 (m, 6H), 6.89–6.59 (m, 2H), 5.60 (s, 1H), 4.42 (t, J = 7.2 Hz, 2H), 4.18 (s, 1H), 3.04 (t, J = 7.2 Hz, 2H). ^{13}C NMR (100 MHz, DMSO-d_6) δ_C (ppm): 172.2, 162.6, 159.2, 155.5, 154.4, 138.0, 133.9, 132.4, 130.9, 129.9, 129.8, 129.1, 128.2, 128.0, 127.8, 127.4, 127.4, 125.8, 123.0, 120.4, 118.9, 108.7, 71.0, 64.1, 51.4, 28.9. HRMS (ESI) m/z: $[M + H]^+$, calcd for $C_{30}H_{23}ClNO_5$: 512.1265, found: 512.1273.

3-(4-Chloro-3-fluorophenyl)-2-(4-(4-chlorophenoxy)phenyl)-1-oxo-1,2,3,4-tetrahydroisoquinoline-4-carboxylic acid (**II13**): white powder, yield 1.19 g (76%), mp 243–245 °C. ^1H NMR (400 MHz, DMSO-d_6) δ_H (ppm): 12.97 (s, 1H), 8.10–8.08 (m, 1H), 7.60–7.51 (m, 3H), 7.45–7.39 (m, 4H), 7.25–7.24 (m, 2H), 7.07–6.97 (m, 5H), 5.63 (d, J = 4.4 Hz, 1H), 4.92 (d, J = 4.4 Hz, 1H). ^{13}C NMR (100 MHz, DMSO-d_6) δ_C (ppm): 170.5, 163.0, 156.6 (d, $^1J_{C-F}$ = 247.0 Hz), 155.5, 154.6, 139.1 (d, $^3J_{C-F}$ = 6.0 Hz), 136.9, 134.1, 132.6, 130.5, 130.0, 129.9, 129.3, 128.9, 128.3, 128.0, 128.0, 127.7, 127.4, 125.4 (d, $^4J_{C-F}$ = 3.0 Hz), 120.5, 120.3, 119.1 (d, $^3J_{C-F}$ = 17.3 Hz), 118.9, 118.8, 116.6 (d, $^2J_{C-F}$ = 21.6 Hz), 63.1, 49.1. HRMS (ESI) m/z: $[M + H]^+$, calcd for $C_{28}H_{19}Cl_2FNO_4$: 522.0675, found: 522.0676.

2-(4-(4-Chlorophenoxy)phenyl)-3-(3,4-dimethoxyphenyl)-1-oxo-1,2,3,4-tetrahydroisoquinoline-4-carboxylic acid (**II14**): white powder, yield 1.25 g (78.6%), mp 238–240 °C. ^1H NMR (400 MHz, DMSO-d_6) δ_H (ppm): 12.98 (s, 1H), 8.08–8.07 (m, 1H), 7.64–7.48 (m, 5H), 7.42–7.40 (m, 2H), 7.24–6.96 (m, 4H), 6.76–6.60 (m, 3H), 5.47 (d, J = 4.0 Hz, 1H), 4.84 (d, J = 4.0 Hz, 1H), 3.66 (s, 3H), 3.51 (s, 3H). ^{13}C NMR (100 MHz, DMSO-d_6) δ_C (ppm): 170.7, 163.1, 155.7, 154.3, 148.3, 147.9, 137.4, 134.6, 132.3, 129.9, 129.3, 127.8, 127.6, 127.3, 120.4, 120.1, 118.8, 111.6, 111.1, 64.0, 55.3, 55.0, 49.4. HRMS (ESI) m/z: $[M + H]^+$, calcd for $C_{30}H_{25}ClNO_6$: 530.1370, found: 530.1379.

2-(4-(4-Chlorophenoxy)phenyl)-3-(3-fluoro-4-methoxyphenyl)-1-oxo-1,2,3,4-tetrahydroisoquinoline-4-carboxylic acid (**II15**): white powder, yield 1.14 g (73.3%), mp 241–244 °C. ^1H NMR (400 MHz, DMSO-d_6) δ_H (ppm): 13.02 (s, 1H), 8.08–8.07 (m, 1H), 7.59–7.41 (m, 5H), 7.22–6.81 (m, 9H), 5.49 (d, J = 3.6 Hz, 1H), 4.88 (d, J = 3.6 Hz, 1H), 3.74 (s, 3H). ^{13}C NMR (100 MHz, DMSO-d_6) δ_C (ppm): 170.6, 163.0, 155.5, 154.5, 150.6 (d, $^1J_{C-F}$ = 243.9 Hz), 146.7 (d, $^3J_{C-F}$ = 10.5 Hz), 137.1, 134.3, 132.5, 129.9, 129.2, 129.0, 127.9, 127.8 (d, $^4J_{C-F}$ = 2.7 Hz), 127.4, 124.4 (d, $^4J_{C-F}$ = 2.6 Hz), 120.3, 118.2, 115.5 (d, $^2J_{C-F}$ = 19.1 Hz), 113.3, 63.3, 55.8, 49.1. HRMS (ESI) m/z: $[M + H]^+$, calcd for $C_{29}H_{22}ClFNO_5$: 518.1171, found: 518.1174.

2-(4-(4-Chlorophenoxy)phenyl)-3-(4-fluoro-3-phenoxyphenyl)-1-oxo-1,2,3,4-tetrahydroisoquinoline-4-carboxylic acid (**II16**): white powder, yield 1.29 g (74.1%), mp 253–255 °C. ^1H NMR (400 MHz, DMSO-d_6) δ_H (ppm): 13.07 (s, 1H), 8.00–7.99 (m, 1H), 7.60–7.58 (m, 2H), 7.48–7.41 (m, 3H), 7.32–7.20 (m, 5H), 7.18–6.97 (m, 6H), 6.87–6.72 (m, 3H), 5.60 (d, J = 4.4 Hz, 1H), 4.84 (d, J = 4.4 Hz, 1H). ^{13}C NMR (100 MHz, DMSO-d_6) δ_C (ppm): 170.6, 163.0, 156.4, 155.5, 154.5, 154.0, 152.0, 142.1, 142.0, 136.9, 134.8, 134.8, 134.4, 132.5, 130.0, 129.9, 129.4, 128.9, 127.9, 127.8, 127.6, 125.3, 125.2, 123.3, 121.9, 120.3, 118.7, 117.0, 116.9, 116.5, 63.2, 49.2. HRMS (ESI) m/z: $[M + H]^+$, calcd for $C_{34}H_{24}ClFNO_5$: 580.1327, found: 580.1322.

3-(4-Bromophenyl)-2-(4-(4-chlorophenoxy)phenyl)-1-oxo-1,2,3,4-tetrahydroisoquinoline-4-carboxylic acid (**II17**): white powder, yield 1.29 g (78.4%), mp 249–251 °C. ^1H NMR (400 MHz, DMSO-d_6) δ_H (ppm): 13.03 (s, 1H), 8.09–8.07 (m, 1H), 7.59–7.58 (m, 2H), 7.43–7.39 (m, 5H), 7.22–7.21 (m, 2H), 7.02–6.96 (m, 6H), 5.54 (d, J = 4.4 Hz, 1H), 4.92 (d, J = 4.4 Hz, 1H). ^{13}C NMR (100 MHz, DMSO-d_6) δ_C (ppm): 170.5, 163.0, 155.5, 154.5, 137.1, 136.7, 134.2, 132.5, 131.1, 130.2, 129.9, 129.9, 129.2, 128.9, 128.6, 128.2, 127.9, 127.8, 127.4, 121.3, 120.4, 120.3, 118.8, 63.7, 49.0. HRMS (ESI) m/z: $[M + H]^+$, calcd for $C_{28}H_{20}BrClNO_4$: 548.0264, found: 548.0254.

2-(4-(4-Chlorophenoxy)phenyl)-3-(4-fluorophenyl)-1-oxo-1,2,3,4-tetrahydroisoquinoline-4-carboxylic acid (**II18**): white powder, yield 1.20 g (82.1%), mp 246–248 °C. ^1H NMR (400 MHz, DMSO-d_6) δ_H (ppm): 13.02 (s, 1H), 8.09–8.08 (m, 1H), 7.60–7.59 (m, 2H), 7.52–7.49 (m, 1H), 7.43–7.41 (m, 2H), 7.21–6.96 (m, 10H), 5.55 (d, J = 4.4 Hz, 1H), 4.91 (d, J = 4.4 Hz, 1H). ^{13}C NMR (100 MHz, DMSO-d_6) δ_C (ppm): 170.5, 163.0, 162.6, 160.7, 155.5, 154.5, 137.1, 134.3, 133.5, 132.4, 130.1, 130.0, 129.9, 129.3, 129.0, 127.9, 127.8, 127.7, 127.4, 120.3, 118.8, 115.1, 114.9, 63.6, 49.1. HRMS (ESI) m/z: $[M + H]^+$, calcd for $C_{28}H_{20}ClFNO_4$: 488.1065, found: 488.1063.

2-(4-(4-Chlorophenoxy)phenyl)-3-(4-chlorophenyl)-1-oxo-1,2,3,4-tetrahydroisoquinoline-4-carboxylic acid (**II19**): white powder, yield 1.22 g (80.9%), mp 248–250 °C. ^1H NMR (400 MHz, DMSO-d_6) δ_H (ppm): 13.09 (s, 1H), 8.10–8.08 (m, 1H), 7.58–7.40 (m, 5H), 7.27–7.21 (s, 4H), 7.09–6.96 (m, 6H), 5.56 (d, J = 4.4 Hz, 1H), 4.93 (d, J = 4.4 Hz, 1H). ^{13}C NMR (100 MHz, DMSO-d_6) δ_C (ppm): 170.5, 163.0, 155.5, 154.5, 137.1, 136.3, 134.2, 132.7, 132.5, 129.9, 129.9, 129.2, 129.0, 128.6, 128.2, 128.2, 127.9, 127.8, 127.5, 127.4, 120.3, 118.8, 63.6, 49.0. HRMS (ESI) *m*/*z*: $[M + H]^+$, calcd for $C_{28}H_{20}Cl_2NO_4$: 504.0769, found: 504.0770.

3-(4-Bromo-3-fluorophenyl)-2-(4-(4-chlorophenoxy)phenyl)-1-oxo-1,2,3,4-tetrahydroisoquinoline-4-carboxylic acid (**II20**): white powder, yield 1.32 g (77.6%), mp 253–255 °C. ^1H NMR (400 MHz, DMSO-d_6) δ_H (ppm): 13.10 (s, 1H), 8.09–8.07 (m, 1H), 7.61–7.51 (m, 4H), 7.42–7.24 (m, 3H), 7.23–7.05 (m, 2H), 7.00–6.87 (m, 5H), 5.61 (d, J = 4.4 Hz, 1H), 4.91 (d, J = 4.4 Hz, 1H). ^{13}C NMR (100 MHz, DMSO-d_6) δ_C (ppm): 170.5, 163.0, 158.6, 156.7, 155.5, 154.6, 136.9, 134.2, 133.3, 132.6, 130.0, 129.9, 129.3, 128.9, 128.9, 128.3, 128.2, 128.0, 128.0, 127.7, 127.4, 125.8, 116.6, 116.4, 107.7, 107.5, 63.1, 49.1. HRMS (ESI) *m*/*z*: $[M + H]^+$, calcd for $C_{28}H_{19}BrClFNO_4$: 566.0170, found: 566.0167.

2.2.2 General procedure for the synthesis of compounds III1–III5. Compound **I23** (1.0 mmol), dicyclohexylcarbodiimide (DCC) (1.1 mmol), hydroxyl substrate (1.1 mmol) and 4-dimethylaminopyridine (DMAP) (3%, molar fraction) were dissolved in 10 mL dry DCM. The reaction mixture was stirred overnight at room temperature. After the completion of the reaction, the resulting mixture was washed with 1% $NaHCO_3$ solution (10 mL × 3), saturated brine, dried over magnesium sulfate, and concentrated under reduced pressure. The organic phase layer was combined, dried over anhydrous Na_2SO_4 and concentrated under reduced pressure. Afterwards, the residue was subjected to column chromatography, eluting with petroleum ether/ethyl acetate (v/v, 15 : 1), to yield ester derivatives **III1–III5**.

Methyl 2-(4-(4-chlorophenoxy)phenyl)-1-oxo-3-phenyl-1,2,3,4-tetrahydroisoquinoline-4-carboxylate (**III1**): white powder, yield 406 mg (83.9%), mp 146–148 °C. ^1H NMR (400 MHz, $CDCl_3$) δ_H (ppm): 8.25–8.22 (m, 1H), 7.46–7.44 (m, 2H), 7.31–7.27 (m, 3H), 7.26–7.18 (m, 5H), 7.16–7.14 (m, 2H), 6.95–6.93 (m, 4H), 5.61 (s, 1H), 4.02 (d, J = 0.8 Hz, 1H), 3.74 (s, 3H). ^{13}C NMR (100 MHz, $CDCl_3$) δ_C (ppm): 171.5, 163.8, 155.9, 155.9, 132.8, 132.5, 130.1, 129.8, 129.7, 129.2, 129.0, 128.8, 128.8, 128.6, 128.4, 126.7, 120.7, 119.4, 65.3, 53.3, 52.0. HRMS (ESI) *m*/*z*: $[M + H]^+$, calcd for $C_{29}H_{23}ClNO_4$: 484.1316, found: 484.1303.

Phenyl 2-(4-(4-chlorophenoxy)phenyl)-1-oxo-3-phenyl-1,2,3,4-tetrahydroisoquinoline-4-carboxylate (**III2**): white powder, yield 465 mg (85.2%), mp 167–169 °C. ^1H NMR (400 MHz, $CDCl_3$) δ_H (ppm): 8.30–8.28 (m, 1H), 7.51–7.49 (m, 2H), 7.36–7.31 (m, 5H), 7.27–7.21 (m, 8H), 7.00–6.98 (m, 2H), 6.94–6.91 (m, 4H), 5.69 (s, 1H), 4.28 (d, J = 0.8 Hz, 1H). ^{13}C NMR (100 MHz, $CDCl_3$) δ_C (ppm): 169.4, 163.4, 155.7, 155.6, 150.5, 138.8, 137.7, 132.7, 131.8, 129.8, 129.6, 129.5, 129.0, 128.9, 128.7, 128.5, 128.4, 128.2, 126.5, 126.4, 121.2, 120.3, 119.1, 64.9, 51.8. HRMS (ESI) *m*/*z*: $[M + H]^+$, calcd for $C_{34}H_{25}ClNO_4$: 546.1472, found: 546.1472.

Benzyl 2-(4-(4-chlorophenoxy)phenyl)-1-oxo-3-phenyl-1,2,3,4-tetrahydroisoquinoline-4-carboxylate (**III3**): white powder, yield 457 mg (81.6%), mp 172–174 °C. ^1H NMR (400 MHz, $CDCl_3$) δ_H (ppm): 8.26–8.24 (m, 1H), 7.45–7.43 (m, 2H), 7.31–7.30 (m, 3H), 7.27–7.25 (m, 2H), 7.22–7.19 (m, 6H), 7.16–7.14 (m, 4H), 6.93–6.92 (m, 2H), 6.87–6.85 (m, 2H), 5.58 (s, 1H), 5.22 (d, J = 8.4 Hz, 1H), 5.16 (d, J = 8.4 Hz, 1H), 4.05 (d, J = 0.8 Hz, 1H). ^{13}C NMR (100 MHz, $CDCl_3$) δ_C (ppm): 170.8, 163.8, 155.9, 155.8, 139.4, 138.0, 135.5, 132.8, 132.5, 130.1, 129.8, 129.8, 129.2, 129.0, 129.0, 128.8, 128.8, 128.80, 128.5, 128.5, 128.4, 126.7, 120.6, 119.4, 67.9, 65.3, 52.2. HRMS (ESI) *m*/*z*: $[M + H]^+$, calcd for $C_{35}H_{27}ClNO_4$: 560.1629, found: 560.1628.

Phenethyl 2-(4-(4-chlorophenoxy)phenyl)-1-oxo-3-phenyl-1,2,3,4-tetrahydroisoquinoline-4-carboxylate (**III4**): light yellow oily liquid, yield 478 mg (83.3%). ^1H NMR (400 MHz, $CDCl_3$) δ_H (ppm): 8.24–8.23 (m, 1H), 7.42–7.40 (m, 2H), 7.27–7.22 (m, 4H), 7.22–7.18 (m, 6H), 7.13–7.10 (m, 3H), 7.02–7.01 (m, 2H), 6.94–6.91 (m, 4H), 5.56 (s, 1H), 4.38–4.33 (m, 2H), 3.96 (d, J = 0.8 Hz, 1H), 2.86 (t, J = 5.2 Hz, 2H). ^{13}C NMR (100 MHz, $CDCl_3$) δ_C (ppm): 170.8, 163.8, 155.9, 155.8, 139.4, 138.1, 137.7, 132.8, 132.5, 130.1, 129.9, 129.7, 129.1, 128.9, 128.9, 128.8, 128.8, 128.7, 128.5, 128.3, 127.0, 126.7, 120.6, 119.4, 66.7, 65.2, 52.1, 35.2. HRMS (ESI) *m*/*z*: $[M + H]^+$, calcd for $C_{36}H_{29}ClNO_4$: 574.1785, found: 574.1784.

Cyclohexyl 2-(4-(4-chlorophenoxy)phenyl)-1-oxo-3-phenyl-1,2,3,4-tetrahydroisoquinoline-4-carboxylate (**III5**): white powder, yield 456 mg (82.7%), mp 158–160 °C. ^1H NMR (400 MHz, $CDCl_3$) δ_H (ppm): 8.24–8.23 (m, 1H), 7.45–7.43 (m, 2H), 7.32–7.30 (m, 2H), 7.27–7.26 (m, 2H), 7.23–7.16 (m, 6H), 6.94–6.92 (m, 4H), 5.61 (s, 1H), 4.86–4.84 (m, 1H), 3.99 (d, J = 0.8 Hz, 1H), 1.77–1.76 (m, 1H), 1.66–1.65 (m, 1H), 1.55–1.45 (m, 1H), 1.44–1.41 (m, 3H), 1.36–1.24 (m, 4H). ^{13}C NMR (100 MHz, $CDCl_3$) δ_C (ppm): 170.4, 163.8, 156.0, 155.7, 133.0, 132.6, 130.0, 129.7, 129.6, 129.1, 128.8, 128.7, 128.7, 128.5, 128.3, 126.8, 120.6, 119.4, 74.4, 65.3, 52.5, 31.6, 31.4, 25.5, 23.5, 23.4. HRMS (ESI) *m*/*z*: $[M + H]^+$ calcd for $C_{34}H_{31}ClNO_4$: 552.1942, found: 552.1939.

2.3 Evaluation of *in vitro* antifungal and antioomycete activities of compounds I1–I34, II1–II20, and III1–III5

The *in vitro* antifungal and antioomycete activities of compounds **I1–I34**, **II1–II20**, and **III1–III5** were determined using the mycelial growth method. The stock solutions of the synthesized compounds (200 mg) were prepared by dissolving them in 800 μL of dimethyl sulfoxide (DMSO) containing 5% *N*,*N*-dimethyl-1-dodecylamine *N*-oxide (OA-12), respectively. The prepared sterile PDA medium was melted by heating to 50 °C and 20 μL of the stock solution was added to the 50 mL of melted PDA medium and they were well-mixed to give the concentration of 100 μg mL^{-1}. The above PDA medium was immediately poured into three sterilized Petri dishes (90 mm diameter). After the medium was solidified, a mycelial disc (5 mm diameter) of the fungal or oomycete isolate listed above was inoculated in the center of each Petri plate. The control group was used by the same treatment with DMSO containing 5% OA-12 without tested compounds. All the plates were incubated at 25 ± 2 °C in darkness for certain days listed in Table 1. Each treatment was replicated three times. The experiment was replicated three times for 7 microorganisms. The mycelial growth diameter (D) was the mean length (mm) of two orthogonal diameter axes passing through the center of the disc. The inhibition rate (I) was calculated by the formula: I (%) = (D_C − D_T)/D_C × 100, where D_C and D_T are the mycelial growth

Table 1 Inhibition rates of compounds **I1–I34** against mycelial growth of 7 phytopathogens at the concentration of 100 μg mL^{-1}[a]

	Inhibition rate (%)						
Compd.	Bo. (6 d)	Fu. (6 d)	Co. (7 d)	Tr. (7 d)	Al. (7 d)	Rh. (3 d)	Py. (2 d)
I1	71.9 ± 2.2	86.7 ± 2.1	86.3 ± 1.0	28.6 ± 1.3	69.2 ± 1.6	96.5 ± 3.5	99.2 ± 0.4
I2	69.6 ± 0.9	70.3 ± 1.4	82.3 ± 0.7	27.8 ± 1.5	66.0 ± 0.9	81.2 ± 1.6	98.4 ± 0.3
I3	70.2 ± 1.0	81.5 ± 0.3	88.3 ± 0.5	39.6 ± 3.3	73.0 ± 1.0	88.4 ± 0.7	99.7 ± 0.3
I4	65.3 ± 0.6	55.1 ± 0.7	76.1 ± 1.1	33.3 ± 3.6	55.3 ± 1.8	55.8 ± 2.1	97.2 ± 0.1
I5	72.2 ± 1.2	82.6 ± 1.2	78.3 ± 0.8	44.9 ± 1.3	71.3 ± 0.5	87.9 ± 2.1	98.9 ± 0.2
I6	72.6 ± 0.7	73.9 ± 2.4	80.4 ± 0.5	39.6 ± 0.7	64.0 ± 3.9	89.8 ± 3.5	98.4 ± 0.1
I7	68.6 ± 1.7	67.5 ± 1.4	79.1 ± 0.4	37.6 ± 0.8	61.7 ± 1.0	93.3 ± 3.4	96.7 ± 0.5
I8	69.6 ± 1.4	64.7 ± 0.4	85.7 ± 0.1	44.4 ± 1.2	71.0 ± 1.2	80.3 ± 2.7	98.3 ± 0.4
I9	72.6 ± 1.3	53.5 ± 2.9	86.5 ± 0.4	41.9 ± 0.5	73.0 ± 1.3	71.5 ± 1.1	98.2 ± 0.2
I10	73.4 ± 1.5	80.6 ± 1.0	86.8 ± 0.3	36.3 ± 1.6	74.5 ± 0.8	79.8 ± 1.2	99.1 ± 0.3
I11	74.5 ± 0.7	72.5 ± 0.7	78.8 ± 0.5	38.3 ± 1.3	65.7 ± 0.3	66.9 ± 1.6	94.7 ± 0.7
I12	71.6 ± 2.4	74.4 ± 1.0	83.8 ± 0.7	39.1 ± 3.0	64.9 ± 0.8	81.4 ± 1.7	96.7 ± 0.2
I13	65.3 ± 1.2	67.0 ± 0.5	84.3 ± 0.4	35.6 ± 1.0	65.4 ± 1.5	79.3 ± 0.3	97.2 ± 0.1
I14	73.5 ± 0.9	73.1 ± 0.9	90.2 ± 0.3	41.4 ± 2.3	71.8 ± 0.8	82.8 ± 1.2	97.3 ± 0.1
I15	68.9 ± 2.0	82.3 ± 1.2	87.5 ± 0.5	44.0 ± 0.4	68.4 ± 1.2	82.2 ± 0.8	98.9 ± 0.3
I16	76.2 ± 0.6	86.8 ± 1.3	92.5 ± 0.1	45.9 ± 1.2	75.0 ± 0.8	81.7 ± 1.5	100.0
I17	74.5 ± 1.7	85.5 ± 0.7	90.3 ± 0.4	44.4 ± 0.8	75.6 ± 3.1	78.7 ± 1.0	99.6 ± 0.1
I18	80.8 ± 0.9	84.8 ± 1.4	89.7 ± 0.5	49.1 ± 1.8	70.7 ± 0.6	90.6 ± 0.7	99.6 ± 0.1
I19	79.2 ± 2.1	90.8 ± 1.0	92.9 ± 0.4	50.1 ± 0.5	74.2 ± 0.3	93.8 ± 1.2	100.0
I20	82.1 ± 0.6	87.6 ± 0.5	93.3 ± 0.8	43.0 ± 1.2	78.5 ± 1.6	73.1 ± 1.0	100.0
I21	74.0 ± 0.4	86.3 ± 0.3	90.3 ± 0.1	39.3 ± 2.8	80.5 ± 1.5	85.7 ± 2.8	100.0
I22	74.5 ± 0.9	78.3 ± 0.3	90.3 ± 0.4	36.5 ± 1.9	71.0 ± 1.8	100.0	100.0
I23	76.4 ± 3.1	87.2 ± 0.4	88.5 ± 0.3	46.9 ± 1.0	81.4 ± 0.8	100.0	100.0
I24	56.4 ± 1.5	37.9 ± 2.6	68.1 ± 1.1	42.3 ± 1.8	66.3 ± 1.3	93.7 ± 10.1	100.0
I25	63.6 ± 2.9	42.7 ± 1.0	73.1 ± 1.5	45.9 ± 3.7	69.5 ± 1.0	77.2 ± 7.8	100.0
I26	59.7 ± 1.2	39.4 ± 0.4	74.6 ± 1.5	42.3 ± 2.1	72.4 ± 0.3	78.6 ± 10.0	100.0
I27	67.6 ± 0.3	39.3 ± 1.7	73.6 ± 2.2	50.0 ± 7.6	74.7 ± 1.3	68.2 ± 4.7	100.0
I28	61.6 ± 0.3	42.3 ± 2.2	65.6 ± 1.6	49.5 ± 2.2	71.8 ± 2.8	76.2 ± 0.6	100.0
I29	55.0 ± 1.2	41.8 ± 0.6	63.4 ± 0.8	46.4 ± 5.8	63.7 ± 2.8	62.5 ± 3.9	97.0 ± 0.4
I30	65.9 ± 1.8	51.4 ± 0.7	77.1 ± 1.0	57.1 ± 6.3	76.2 ± 1.1	69.4 ± 2.8	100.0
I31	60.2 ± 1.6	41.4 ± 2.1	64.6 ± 0.3	52.2 ± 6.3	70.7 ± 1.1	83.2 ± 10.1	98.8 ± 0.7
I32	57.7 ± 1.4	42.7 ± 0.7	64.1 ± 0.1	53.3 ± 4.0	66.6 ± 0.6	67.7 ± 0.6	100.0
I33	63.6 ± 1.6	41.4 ± 1.3	68.2 ± 0.2	41.6 ± 0.5	67.5 ± 1.1	94.5 ± 1.4	98.3 ± 0.3
I34	60.6 ± 1.2	40.4 ± 0.5	68.9 ± 1.6	47.9 ± 1.8	64.0 ± 1.8	85.7 ± 5.8	95.9 ± 0.1

[a] Bo.: *Botrytis cinerea*; Fu.: *Fusarium oxysporum* f. sp. *niveum*; Co.: *Colletotrichum gloeosporioides*; Tr.: *Trichothecium roseum*; Al.: *Alternaria mali*; Rh.: *Rhizoctonia solani*; Py.: *Pythium recalcitrans*. The number of days in each bracket is the culture duration of the strains on PDA plates before measuring the diameters of mycelial colonies. The data in the table are expressed as the mean ± standard error of mean (SEM) ($n = 3$).

diameters of the control and treatment groups, respectively. The result was presented as the mean value of three independent replicates ± standard error of the mean (SEM).

To obtain the toxicity of the compounds, 2 mg, 5 mg, 10 mg, 20 mg, 40 mg, 100 mg and 200 mg of each test compound were dissolved in 800 μL of DMSO containing 5% OA-12, respectively. The following mix of stock solution (20 μL) with PDA medium (50 mL) rendered the concentrations of 1 μg mL^{-1}, 2 μg mL^{-1}, 5 μg mL^{-1}, 10 μg mL^{-1}, 20 μg mL^{-1}, 50 μg mL^{-1} and 100 μg mL^{-1}. The following operations were performed by following the same procedures described above. The inhibition rate of each concentration was calculated. The concentration was log-transformed value (y) and the inhibition rate was transformed into probit value (x). A linear regression equation was obtained by fitting y against x using Microsoft Excel 2013 and the median effective concentration value (EC_{50}) was calculated from the obtained equation. The experiment was replicated three times and the result was presented as the mean value of three independent replicates ± SD.

2.4 Evaluating *in vivo* control efficacy of compound I23 against *P. recalcitrans* by the pot experiment

Nicotiana benthamiana was used to evaluate *in vivo* control efficacy of compound **I23** against *P. recalcitrans*. The PINDSTRUP substrate (Pindstrup, Denmark) and vermiculite in a 2 : 1 ratio were mixed thoroughly and autoclaved at 120 °C for 4 h to give a sterile mixture. The *N. benthamiana* seeds were planted using the above mixed soil in plastic pots (top diameter × height × bottom diameter, 10 cm × 7 cm × 7 cm). All of the pots were placed in a greenhouse at 25 °C under ambient light. After 3 weeks of planting, 50 mL of the **I23** solutions containing active ingredients (a.i) of 1.0 mg, 2.0 mg and 5.0 mg were applied into shallow circular trenches around the base of the *N. benthamiana* seedlings, respectively. In the preventive assay, after 1 day of treatment, 50 mL of a mycelial solution of *P. recalcitrans* (three 5 mm pellets inoculated in PDB at 25 °C in darkness for 2 d with a shaking speed of 120 rpm) was inoculated into the same shallow circular trench. In the curative assay, the mycelial solution was inoculated 2 d before the treatment of **I23** solution. Two *N. benthamiana* plants were in each pot and each treatment contained 10 pots. After 1 week, the diseased plants were counted for each treatment. The incidence of disease (ID%) of each treatment was calculated by the following formula: (the number of diseased plants)/20 × 100. The experiment was repeated three times and the results were expressed as the mean ± SEM of three independent replicates.

2.5 Three-dimensional quantitative structure–activity relationship (3D-QSAR) analysis

The biological activities (EC_{50} (mM)) in Table 2 were transformed into pEC_{50} ($-\log EC_{50}$). 3D structures of all the compounds were constructed using Sybyl X-2.1 software and they were energy minimized using Tripos force field with Powell conjugate gradient descent method (max iterations of 1000 and a convergence criterion of 0.05 kcal mol^{-1} $Å^{-1}$). Meanwhile, Gasteiger–Huckel charges were added to the molecules. Compounds were ranked in descending order by their pEC_{50} values and the fourth, eighth, twelfth, …, were picked out as the test set (compounds **I1**, **I3**, **I8**, **I14**, **I15**, **I17**, **I30**, **II1**, **II5**, **II12**, **II15**, **II16**, **II19** and **III4**). The remaining compounds were used as the training set. The molecular alignment was performed using the common backbone of the most potent compound **I23** and the result was shown in Fig. S1.†

Table 2 The toxicity of compounds I1–I34, II1–II20 and III1–III5 against mycelial growth of *P. recalcitrans* (2 d)[a]

Compd.	EC_{50} (μM)	Compd.	EC_{50} (μM)
I1	46.6 ± 2.9	**I32**	26.9 ± 0.3
I2	45.8 ± 2.3	**I33**	43.1 ± 0.8
I3	29.5 ± 2.0	**I34**	40.9 ± 2.3
I4	45.4 ± 2.8	**II1**	18.2 ± 0.2
I5	53.7 ± 1.0	**II2**	27.7 ± 0.1
I6	46.8 ± 2.6	**II3**	32.0 ± 0.5
I7	43.6 ± 0.5	**II4**	38.5 ± 1.8
I8	59.8 ± 0.6	**II5**	45.3 ± 2.6
I9	57.4 ± 0.5	**II6**	43.0 ± 2.0
I10	54.0 ± 0.7	**II7**	31.5 ± 5.4
I11	46.5 ± 2.1	**II8**	47.1 ± 1.5
I12	67.8 ± 0.1	**II9**	31.3 ± 2.3
I13	65.1 ± 0.1	**II10**	41.3 ± 0.2
I14	40.6 ± 1.5	**II11**	16.9 ± 0.4
I15	42.8 ± 0.7	**II12**	35.8 ± 3.2
I16	20.9 ± 0.2	**II13**	29.6 ± 0.4
I17	23.2 ± 1.1	**II14**	47.8 ± 1.1
I18	25.1 ± 1.7	**II15**	31.3 ± 0.1
I19	21.5 ± 0.5	**II16**	48.7 ± 0.9
I20	23.2 ± 1.0	**II17**	30.3 ± 0.3
I21	14.7 ± 0.3	**II18**	33.1 ± 0.1
I22	20.8 ± 0.1	**II19**	32.2 ± 0.1
I23	14.0 ± 0.3	**II20**	34.0 ± 2.8
I24	38.9 ± 4.0	**III1**	951.4 ± 41.4
I25	33.2 ± 1.1	**III2**	1258.1 ± 76.3
I26	29.6 ± 1.9	**III3**	874.3 ± 65.2
I27	26.0 ± 0.1	**III4**	895.7 ± 58.7
I28	29.4 ± 1.2	**III5**	1055.2 ± 80.1
I29	41.7 ± 3.5	Hymexazol	37.7 ± 3.8
I30	26.0 ± 0.6	Dimethomorph	>258.4
I31	36.3 ± 2.7		

[a] The data in the table are presented as the mean ± standard derivation (SD) of three repeated experiments.

For CoMFA studies, a cubic lattice with a grid spacing of 4.0 Å was generated to calculate steric and electrostatic fields using the sp^3 hybridized carbon as the probe atom with a +1.0 charge. Cut-off values for both fields were set to 30.0 kcal mol^{-1}. For CoMSIA studies, the same lattice with the parameters (probe atom with a +1.0 charge and attenuation factor of 0.3) was used to calculate steric and electrostatic, hydrophobic, and hydrogen bond donor and acceptor fields.

For the partial least squares (PLS) analysis, the leave-one-out (LOO) method was used to carry out a cross-validation analysis, giving the square of the cross-validation coefficient (q_{cv}^2) and the optimum number of components (N_{opt}). Using N_{opt}, a final model was generated with the non-cross-validated correlation coefficient (r_{ncv}^2), standard error of estimation (SEE_{ncv}), and *F*-test value (*F*) using Sybyl software.

For the test set, the predictive correlation coefficient (r_{test}^2) was calculated using the following formula:

$$r_{test}^2 = 1 - \frac{\sum\left(Y_{pred} - Y_{exp}\right)^2}{\sum\left(Y_{exp} - Y_{mean}\right)^2}$$

where Y_{pred}, Y_{exp} and Y_{mean} are the predictive activities of the test set, the experimental activities of the test set and the mean activity of the training set. The standard error of predication of test set (SEE_{test}) was calculated using the following formula:

$$SEP_{test} = \sqrt{\frac{\sum\left(Y_{pred} - Y_{exp}\right)^2}{n}}$$

where *n* is the number of samples in the test set.

2.6 Effects of I23 on cell membrane permeability of P. recalcitrans

Ten mycelial plugs taken from the edge of a 2-day-old colony of *P. recalcitrans* on PDA plates were transferred to 150 mL of PDB in a 250 mL flask. After incubation on a shaker (120 rpm in darkness at 25 °C) for 2 d, compound **I23** was added to obtain the concentrations of 8.7 μM (EC_{30}), 14.0 μM (EC_{50}) and 20.0 μM (EC_{70}). After shaking for a further 12 h, the mycelia were collected by two layers of filter paper and washed with distilled water three times. Afterward, 0.2 g mycelia of *P. recalcitrans* were suspended in 20 mL distilled water in a 20 mL centrifuge tube and the electrical conductivity of the suspensions was measured after 0, 0.5, 1, 2, 4, and 6 h using a laboratory conductivity meter digital conductivity meter (DDS-318, Shanghai Leici Xinjing Instrument Co., Ltd., China). At last, the mycelia were boiled for 5 min and the final electrical conductivity (σ_f) was recorded. The relative conductivity at different times was calculated by $\sigma_t/\sigma_f \times 100$, where σ_t is the electrical conductivity at different times. The experiment was repeated three times.

2.7 Fluorescence microscopy observation

The vital dye FM4-64 (Catalog number: T13320, Invitrogen™, Thermo Fisher Scientific Inc.) was used to stain membrane systems of mycelia of *P. recalcitrans*. The mycelia of *P.*

recalcitrans were collected from the above PDB after shaking for a further 12 h. Then, the mycelia were placed on a slide and a drop of FM4-64 (Catalog number: T13320, Invitrogen™, Thermo Fisher Scientific Inc.) working solution (10 μM) or JC-1 (Catalog number: C2005, Beyotime Biotechnology, China) working solution (10 μM) was added. The slice was then covered with a coverslip, and the samples were kept at room temperature in the dark for 10 min and analyzed using an Olympus IX71 inverted fluorescent microscope. Images were obtained using DP2-BSW software.

2.8 Transmission electron microscopy (TEM) observation

The apical portions of the mycelial pellets from the above PDB after shaking for a further 12 h were cut and fixed in 2.5% glutaraldehyde at 4 °C overnight. Then samples were washed twice with 0.1 M PBS (pH 7.0), were post-fixed in 1% osmium tetroxide for 2 h, and washed twice with 0.1 M PBS (pH 7.0) again. After that, samples were dehydrated in an ascending ethanol series (30, 50, 70, 80, 90 and 100%, v/v) for 15 min each concentration. Subsequently, samples were embedded in Spurr resin and polymerized at 70 °C overnight. Blocks were sectioned (80 nm) using a LEICA EM UC7 ultratome (Leica UC7) and the sections were mounted on copper grids. Staining was performed with uranyl acetate and alkaline lead citrate for 10 min, respectively. Finally, micrographs were obtained using a transmission electron microscope (Hitachi Model H-7650, Tokyo, Japan) at an accelerating voltage of 80 kV.

2.9 Lipidomics analysis

The mycelia of *P. recalcitrans* were collected from the above PDB after shaking for a further 6 h. The control and the treated groups contained each four independent replicates. Lipid extraction was followed the reported MTBE method.[25] Briefly, appropriate amount of internal lipid standards were added to the samples and then they were homogenized with 200 μL H_2O and 240 μL CH_3OH. After that, 800 μL of MTBE was added and the mixture was ultrasound for 20 min at 4 °C followed by continually sitting for 30 min at room temperature. The obtained solution was subjected to centrifugation separation (14 000 *g* for 15 min at 10 °C) to give the upper organic solvent layer, which was dried under nitrogen atmosphere.

The lipid absolute quantification analysis was performed using liquid chromatography with tandem mass spectrometry (LC-MS-MS) method. Reverse phase chromatography was used for LC separation (charged surface hybrid C18 column: pore size 130 Å, particle size 1.7 μm, 2.1 mm × 100 mm, Waters). The eluting solution A was comprised of CH_3CN/H_2O (6 : 4, v/v) with 0.1% formic acid and 0.1 Mm ammonium formate and B was comprised of CH_3CN/isopropanol (1 : 9, v/v) with 0.1% formic acid and 0.1 Mm ammonium formate. In brief, the lipid extract solutions (in 200 μL 90% isopropanol/CH_3CN) were centrifuged at 14 000 *g* for 15 min at 10 °C. An aliquot of 3.0 μL of sample was injected into the chromatographic instrument. The initial eluting solvent system was 30% B in A at a flow rate of 300 μL min^{-1}. It was kept for 2 min, and then linearly increased to 100% solvent B in 23 min, followed by equilibrating at 5% solvent B for 10 min. MS was carried out by Q-Exactive Plus in positive and negative mode, respectively. ESI parameters were optimized and preset for all measurements as follows: source temperature, 300 °C; capillary temperature, 350 °C; the ion spray voltage, 3000 V; S-Lens RF level, 50%; and the scan range, *m*/*z* 200–1800.

Lipid Search, a search engine, was used for the identification of lipid species based on MS/MS math. Lipid Search contains more than 30 lipid classes and more than 1 500 000 fragment ions in the database. Both mass tolerance for precursor and fragment were set to 5 ppm.

2.10 Statistical analysis

A one-way analysis of variance (ANOVA) was used for the statistical analysis using the software of SPSS 16.0 software package. Data were expressed as mean standard error of the mean (SEM) and compared using a Fisher's least-significant difference test at the 95% confidence interval.

3. Results & discussion

3.1 Synthesis of 3,4-dihydroisoquinolin-1(2*H*)-one derivatives

The reaction of imines with homophthalic anhydride in refluxing dry toluene is outlined in general terms in Scheme 1. The imines were prepared *in situ* by condensation of the aromatic aldehydes with aliphatic and aromatic amines in anhydrous DCM using anhydrous Na_2SO_4 as desiccant agent. The imine intermediates are unstable and were therefore not isolated but used immediately in the subsequent CCR to afford the desired isoquinolinic acids **I1–I34** and **II1–II20**. The imines employed in the present study generally resulted in good to excellent isolated product yields. Noticeably, in our unsuccessful cases, when the *ortho*-substituted aromatic amines were *o*-toluidine, 2-ethylaniline, 2-phenoxyaniline, 2-benzylaniline, 2-fluoroaniline, 2,3-dimethylaniline, 2,6-dimethylaniline, the corresponding products could not be obtained from the reaction system, suggesting that the CCR has a limited tolerance for the *ortho*-substituted aromatic amines. Remarkably, there is scarce literature that employs the substrates of *ortho*-substituted aromatic amines in CCR. Esters **III1–III5** were readily synthesized by reaction of compound **I23** with the corresponding hydroxyl substrates using DCC as a coupling reagent with yields higher than 80% (Scheme 2).

Generally, the CCR generates racemic products. The relative configuration assignment was initially performed on the basis of the chemical shifts of H-4 and the coupling constants between H-3 and H-4. The high field signals (<4.30 ppm) were found for the H-4 signals of 3-phenyl *trans*-diastereomers, while the relative low field signals (>4.50 ppm) occurred for the *cis*-isomers.[24,26–29] According to the reported molecular models,[24,26–28] this might be ascribed to the shielded effects of the aromatic cloud on H-4 of *trans*-isomers. Meanwhile, a relative larger H-3/H-4 coupling constant of *cis*-diastereomers usually occurred higher than 4.0 Hz (Fig. 2). Conversely, *trans*-configured products generally show H-3/H-4 coupling constant

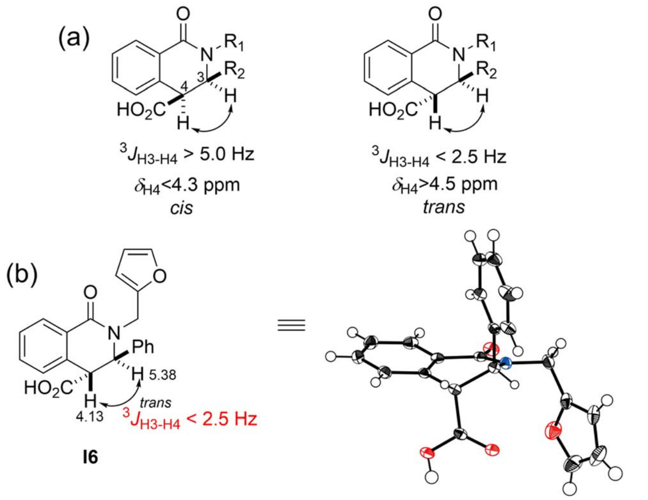

Fig. 2 The reported δ_{H4} values and H-3/H-4 coupling constants of *cis*- and *trans*-diastereomers of 3-phenyl tetrahydroisoquinolone-4-carboxylic acid compounds (a); and the δ_{H4} value and H-3/H-4 coupling constant of *cis*-**I6** and its single-crystal structure (CCDC Deposition No. 2180985†) (b).

of less than 2.5 Hz. The relative configuration analysis of *trans*-**I6** was exemplified *via* its single-crystal X-ray results (Fig. 2 and Table S1†). Thereby, compounds **I4**, **I5–I21**, **I23**, **I24**, **I26–I34**, **II1–II3**, **II5**, **II7**, **II8**, **II11**, **II14–II16**, and **II18** were obtained predominantly as a single and racemic *cis*-isomer. However, the only *trans*-isomer was formed for compounds **I1–I3**, **I5–I8**, **I10–I14**, **I22**, **II12**, and **III1–III5**, since their H-3/H-4 signals appeared singlet (or unresolved doublets). Collectively, the relative configuration ratios of the other compounds were shown in Table S2.† Particularly notable is the configuration inversion of the *trans*-esters **III1–III5** from *cis*-**I23**. It has been demonstrated that the base could promote totally isomerization of *cis*- to *trans*-configuration when *cis*-products of CCR were exposed to aqueous NaOH solution[30] or the organic base *N*,*N'*-carbonyldiimidazole (CDI) was used in the *trans*-ester synthesis from the *cis*-precursor.[21] The *cis*-products of CCR are conceived as the kinetic products and they were removed from the reaction system by precipitation at room temperature and the isomerization to more stable *trans*-configured counterpart might occur under some conditions, such as the existence of bases. In the present study, we found the general coupling reagent DCC could lead to the configuration inversion as well.

3.2 *In vitro* antifungal and antioomycete activities of 3,4-dihydroisoquinolin-1(2*H*)-one derivatives

Firstly, 7 phytopathogens were used to determine the *in vitro* antifungal and antioomycete activities of compounds **I1–I34** against mycelial growth at the concentration of 100 μg mL^{-1}. As shown in Table 1, in spite of their broad spectrum of bioactivities, they varied in activity against different pathogens. Generally, **I1–I34** showed much better activity against oomycete *P. recalcitrans* than other 6 fungi, with all the inhibition rates higher than 95%. Meanwhile, the inhibition rates of the title compounds against *B. cinerea*, *F. oxysporum* f. sp. *niveum*, *C. gloeosporioides*, *T. roseum*, *A. mali* and *R. solani* were within the range of 55%–82.1%, 37.9%–90.8%, 63.4%–93.3%, 27.8%–57.1%, 55.3%–81.4%, and 55.8%–100%, respectively. Considering the distinguished differences between oomycetes and fungi and the conspicuous activity of **I1–I34** against *P. recalcitrans*, we chose *P. recalcitrans* as the target strain for the following toxicity assay and SAR analysis.

It is noteworthy that the oomycete *P. recalcitrans* is a soil-borne phytopathogen with a wide host-range, such as tobacco,[31] soybean,[32] corn,[33] alfalfa,[34] grape, beet[35] and carrot,[36] causing seed decay, seedling collapse and root rot, cavity spot, and significantly reducing crop yield. Due to its easy recovery profile from flooding soil[37] and insensitivity to many commercial fungicides,[33,36] there is a need for exploring effective anti-oomycete agents to control this pathogen. The toxicity of compounds **I1–I34,II1–II20** and **III1–III5** against mycelial growth of *P. recalcitrans* was further determined and the results were shown in Table 2. **I23** stood out as the most potent activity with the EC_{50} value of 14.0 μM (Fig. S2†), which was superior over hymexazol (EC_{50} = 37.7 μM) and dimethomorph (EC_{50} > 258.4 μM). Generally, the EC_{50} values of 4-carboxyl derivatives **I1–I34** and **II1–II20** ranged from 14.0 μM to 67.8 μM. Nevertheless, loss of a free carboxyl group (**III1–III5**) triggered a significant decrease in toxicity, indicating the necessity of unsubstituted carboxyl group for the activity.

3.3 3D-QSAR analysis

3.3.1 Statistical data of the optimal 3D-QSAR models. A division of 45 compounds as training set and 14 compounds as test set was used for establishing and externally validating the 3D-QSAR models, respectively. The statistical data of the optimal 3D-QSAR models are summarized in Table 3. The CoMFA model exhibits a q_{cv}^2 value of 0.609 with N_{opt} of 4, r_{ncv}^2 of 0.940, SEE_{ncv} of 0.111, and *F*-statistic value of 171.652. The contribution of the steric and electrostatic fields were 58.1% and 41.9%, respectively, implying the key role of steric field in CoMFA model. The CoMSIA model shows a q_{cv}^2 value of 0.711 with N_{opt} of 5, r_{ncv}^2 of 0.945, SEE_{ncv} of 0.107, and *F*-statistic value of 147.469. Steric, electrostatic, hydrophobic, H-bond donor and H-bond acceptor fields contribute 11.0%, 18.7%, 17.8%,

Table 3 Statistical data of the optimal QSAR models[a]

Parameters	CoMFA	CoMSIA
q_{cv}^2	0.609	0.711
N_{opt}	4	5
$r_{ncv}2$	0.940	0.945
SEE_{ncv}	0.111	0.107
F-value	171.652	147.469
r_{test}^2	0.989	0.989
SEP_{test}	0.130	0.131
Steric	0.581	0.110
Electrostatic	0.419	0.187
Hydrophobic	—	0.178
H-bond donor	—	0.135
H-bond acceptor	—	0.391

[a] "—" indicates that the data has not been determined.

13.5% and 39.1%, respectively, indicating the important role of H-bond acceptor field in the CoMSIA model.

The internal validation parameters revealed that these two models were statistically significant of predicating the activity. As shown in Fig. S3,† the actual and predicated pEC_{50} values of the training and test set molecules (Table S3†) were strongly correlated in a linear fashion. Meanwhile, the external validation parameters of the test set reflect the good predicative capacity of the models. The r_{test}^2 (and SEP_{test}) of the CoMFA and CoMSIA models were 0.989 (0.130) and 0.989 (0.131), respectively.

3.3.2. 3D-QSAR contour map analysis. To get insights into the effects of different fields on activity in a structure-based manner, contour maps (Fig. 3) generated from CoMFA and CoMSIA models were analyzed by displaying the regions in which the energy variations of the molecular fields were consistent with changes in bioactivity.

In the steric contour maps of CoMFA model (Fig. 3a), it can be observed that a big green contour was near the N2 site, indicating that bulky groups at that position might be more favorable for the activity. This was identical with the following experimental results: **I21** (R_1 = 4-$C_6H_5C_6H_4$) > **I16** (4-$CH_3(CH_2)_3C_6H_4$) > **I15** (C_6H_5) > **I1** ($(CH_2)_3CH_3$) ≈ **I11** (cyclopropyl), **I28** (4-$CF_3OC_6H_4$) > **I33** (4-$OCHF_2C_6H_4$), **II13** (3-F,4-ClC_6H_3) > **II19** (4-ClC_6H_4). The other two big yellow contour regions around the phenyl group at C3 site and the carboxyl group at C4 site suggest that bulky groups at those sites furnish negative effects to the bioactivity. This could be exemplified by the comparison of compounds **I23** and **II1–II20**. Meanwhile, the above analysis have confirmed that the substitution of carboxyl group at C4 site significantly decreased the activity. It is found that a blue contour map overlaid on the *para*-position of the C-3 phenyl group in the electrostatic contour maps (Fig. 3b), signifying that the superior substituents at that site should cause fairly lesser electron density. The situation can be proved by the activity order: **II1** (R_2 = 4$(CH_3)_2CHC_6H_4$) > **II2** (4-$(CH_3)_3CC_6H_4$) > **II17** (4-BrC_6H_4). The presence of a red block near the *meta*-position of the C-3 phenyl group denotes that the electron-rich substituents attached there are harmful to activity, for instances, **II15** (R_2 = 3-F,4-$CH_3OC_6H_3$) > **II14** (3,4-di$CH_3OC_6H_3$) and **II13** (3-F,4-ClC_6H_3) > **II19** (4-ClC_6H_4).

As shown in Fig. 3c, the steric and electrostatic contour maps of the CoMSIA model are similar to those of the CoMFA model, showing the similar trends of the influences of these two fields on activity in the CoMSIA model. For the hydrophobic field (Fig. 3d), most of the yellow contour is covered around R_1 and R_2 groups, revealing that the general hydrophobic substituents are advantageous. Besides, it is well known that the hydrophobicity would enhance with the increase of the alkane chain length, which is consistent with the sequences of activity: **I3** (R_1 = $(CH_2)_7CH_3$) > **I1** ($(CH_2)_3CH_3$) and **I10** ($(CH_2)_3C_6H_5$) > **I9** ($(CH_2)_2C_6H_5$) > **I8** ($CH_2C_6H_5$). This may also explain that compounds with hydrophobic substituent such as –X (**I24–I27**, **II13**, and **II17–II20**), alkyl (**I16**, **I17**, **I21**, **I22**, and **II1–II3**) and ether group (**I18** and **II7**) at these positions possess the desirable activity.

The hydrogen bond donor contour map (Fig. 3e) identifies a purple contour at the N2 position, implying that the R_2 groups with H-bond donor are not welcome. Simultaneously, a magenta region near the same sites in hydrogen bond acceptor contour map (Fig. 3e) suggests that compounds with H-bond acceptor can ameliorate the activity, which is basically in line with the circumstance reflected in the H-bond donor field. The potency of compound **II15** (R_2 = 3-F,4-$CH_3OC_6H_3$) with an H-bond acceptor at this site was raised compared with compound **II5** (4-$CH_3OC_6H_4$). On the contrary, the red

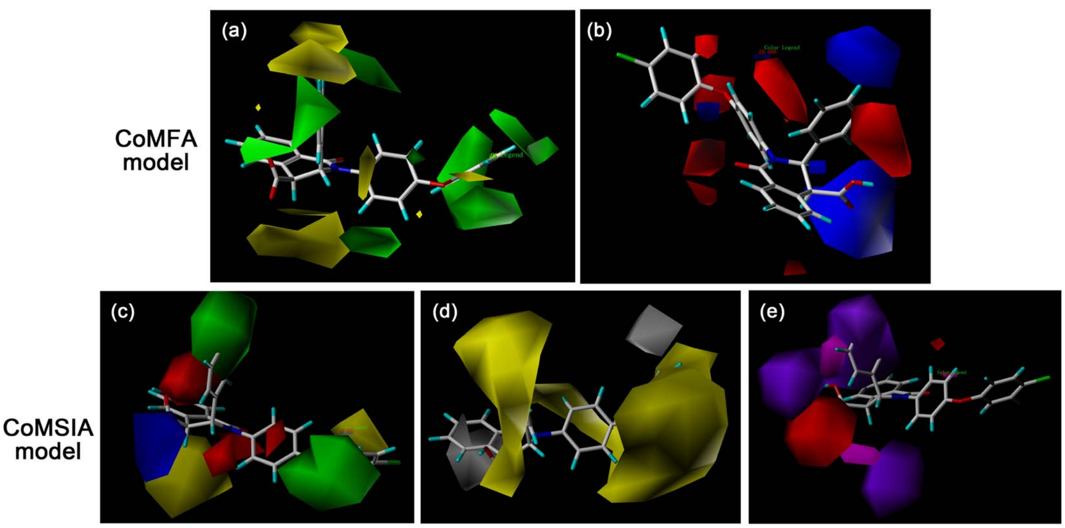

Fig. 3 The view of CoMFA (a and b) and CoMSIA (c–e) StDev × Coeff contour maps visualized based on the most potent compound **I23**. (a) The steric contour map. Green (favored) and yellow (disfavored) colors represent 80% and 20% level contributions, respectively. (b) The electrostatic map. Blue (favored, electropositive): 80%; red (disfavored, electronegative): 20%. (c) The steric contour map [green (favored): 80%; yellow (disfavored): 20%] and electrostatic contour map [blue (favored, electropositive): 80%; red (disfavored, electronegative): 20%]. (d) The hydrophobic contour map. Yellow (favored, hydrophobic): 80%; white (disfavored, hydrophilic): 20%. (e) The hydrogen bond donor contour map [cyan (favored): 80%; purple (disfavored): 20%] and hydrogen bond acceptor contour map [magenta (favored): 80%; red (disfavored): 20%].

polyhedron is nearest to the C4 position, suggesting that compounds **I** and **II** series with H-bond donor (R_3 = H) have fantastic activity than esterified compounds.

3.4 Control efficacy of compound I23 in pot experiment

The control efficacy of compound **I23** against *P. recalcitrans* on tobacco seedlings was determined by the pot experiment. As shown in Fig. 4, *P. recalcitrans* caused the obvious damping-off and plant shriveling of infected tobacco seedlings in the control group and **I23**-treated group (1.0 mg per pot), while the undiseased seedlings were healthy and vigorous. As can be seen from Table S4,† the preventive efficacy was superior over the curative efficacy, indicating that taking preventive measures to reduce is more effective to control the disease caused by *P. recalcitrans* before the onset of the disease outbreak. In practice, just like the common saying 'an ounce of prevention is worth a pound of cure', the preventive means, such as fungicide seed treatment, is a common and effective practice to control soilborne diseases worldwide in agriculture.[38] Meanwhile, both of these control efficacies were improved with the applied dose of **I23** being increased. Particularly, at the dose of 2.0 mg per pot, the preventive and curative efficacies of **I23** were 75.4% and 33.3%, respectively, which did not show significant differences with those of hymexazol treatments. When the dose was 5.0 mg per pot, **I23** achieved an obvious increase in the preventive efficacy (96.5%). These results demonstrated that compound **I23** is a promising antioomycete agent to control the disease caused by *P. recalcitrans*.

3.5 Effects of compound I23 on *P. recalcitrans*

As aforementioned by the 3D-QSAR analysis, the C4 carboxyl group is of great importance to the scaffold **1** and apparently the functional carboxylic acids represents their intrinsic profile of organic acid. Given the well-established fact that acid stress could result in the damaged lipidic cytoplasm membrane and decreased membrane fluidity,[39] the impact of compound **I23** on the cell membrane permeability of *P. recalcitrans* was evaluated. As can be seen from Fig. S4,† **I23** caused the increase of the relative electrical conductivity at its EC_{30} (8.7 μM), EC_{50} (14.0 μM) and EC_{70} (20.0 μM), which was concentration-dependent. These results revealed that **I23** impaired cell membrane integrity of *P. recalcitrans*, leading to the easy leakage of intracellular electrolytes and thus enhancing the relative electrical conductivity. Interestingly, it has also been found that cinnamic acid, a known small antifungal molecular organic acid, could significantly increase cell membrane permeability of *Sclerotinia sclerotiorum* (Lib.) de Bary.[40]

Notely, when *P. recalcitrans* was exposed to the EC_{50} and EC_{70}, their relative electrical conductivities were significantly greater than those of the EC_{30} and the control. Therefore, the EC_{50} was chosen to detect the effect of **I23** on the ultrastructural changes of *P. recalcitrans* by TEM. The untreated control

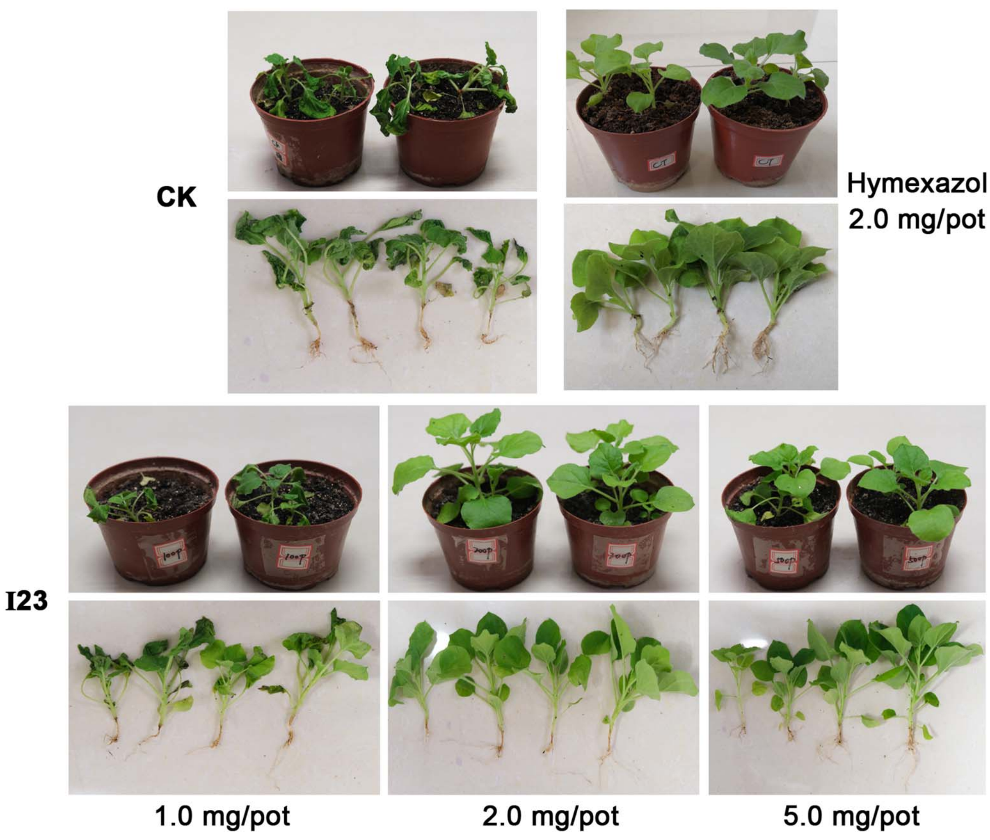

Fig. 4 Representative photos of the preventive effect results of I23 (1.0 mg per pot, 2.0 mg per pot and 5.0 mg per pot) against *P. recalcitrans* in *Nicotiana benthamiana* in pot experiment. Hymexazol (2.0 mg per pot) was used as the positive control.

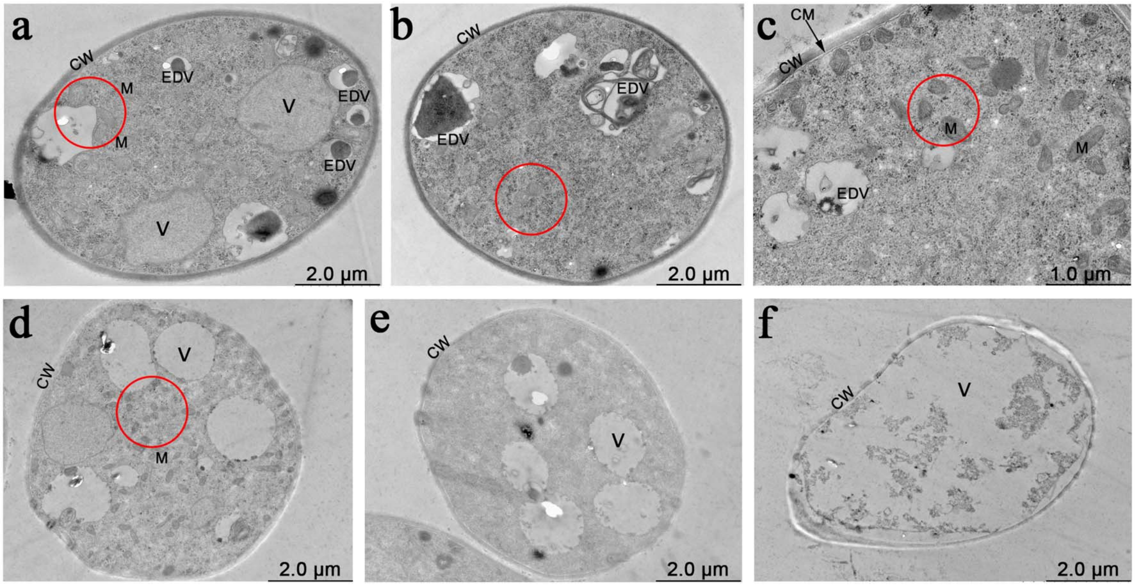

Fig. 5 Transmission electron microscopy (TEM) photos of *P. recalcitrans* treated with **I23**. The control group (a–c) and the **I23**-treated group (d–f) at its EC_{50}. EDV, electron-dense vesicles; M, mitochondria; V, vacuoles; CW, cell wall; CM, cytoplasm membrane. The size of mitochondria in the treated cells were shrunk (in the red circle in d) compared with the untreated (in the red circles in a–c).

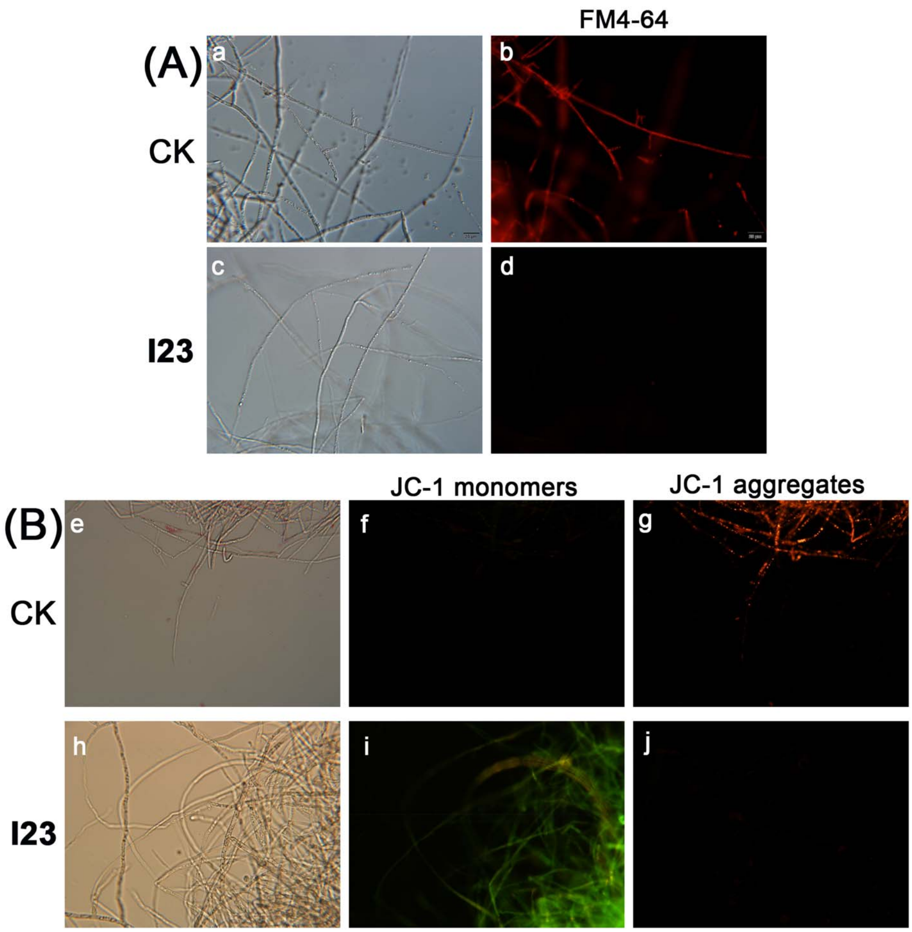

Fig. 6 The fluorescence microscopy photos of *S. sclerotiorum* mycelia stained by FM4-64 (A) and JC-1 dyes (B).

remained intactness of cellular ultrastructures, including dense and even cell walls, clear and complete plasma membranes, mitochondria with visible cristae, distinct electron-dense vesicles (EDVs) and organelles (Fig. 5a–c). After treatment with **I23** at the EC_{50}, moderate to extreme ultrastructural alternations occurred in the cells of *P. recalcitrans*. The density of the cell walls decreased and the membranous organelles became disorganized, with abnormal and indiscernable morphologies. Conspicuously, mitochondrial size was reduced and the incidence of empty vacuoles increased compared with those of cells from the untreated control (Fig. 5d and e). Even worse, the organelles degraded severely, the cell walls were not intact, and the inner wall layer of the original hyphae was retracted into cell lumen (Fig. 5f). Considering the ultrastructural changes of the cellular membranous systems, it is supposed that **I23** had profound impacts on the biological membrane.

These impacts could be exemplified by the FM4-64 staining and mitochondrial membrane potential vanishing by JC-1 staining as well. The lipophilic vital styryl dye FM4-64 primarily stains the plasma membrane, endosomes and vesicles in the untreated fine cells of *P. recalcitrans* (Fig. 6Aa and b). In contrast, after *P. recalcitrans* was treated with **I23** at the EC_{50} for 12 h, no definitive staining pattern was observed either at the plasma membrane or in the cytosol, up to 60 min after exposure to the dye (Fig. 6Ac and d). Further JC-1 staining showed that the decreasing and vanishing status of mitochondrial membrane potential occurred as early as 6 h post-treatment (Fig. 6B), indicating the mitochondria damaged or dead states. As a matter of fact, it has been found that organic acids could serve as uncouplers that generally dissipate pH and electrical gradients across biological membranes.[41] Taken together, it has been speculated that **I23** might exert the anti-oomycete activity against *P. recalcitrans* by interfering with cytoplasmic membrane structure and membrane proteins or membrane uncoupling capabilities.

3.6 Lipidomics analysis

As is known, a lipid bilayer is the foundational part of all cellular membranes. In order to gain an insight into the effects of **I23** on the biological membranes of *P. recalcitrans*, lipidomics strategy was carried out to identify and quantify the lipid constituents of the control and the **I23**-treated groups, respectively. A total of 1685 individual lipid species were quantified; these include different glycerophospholipid, sphingolipid, sterol lipid, prenol lipid, fatty acyl, and saccharolipid classes (Fig. 7a and b). Generally, the basic lipid bilayer is composed of three main types of lipids—phospholipids, sphingolipids, and cholesterol, in which glycerophospholipid serves as a basically structural component of cell membranes.[42,43] The results of the lipid composition analysis indicated that **I23** did not alter the composition of the membraneous lipids but caused their proportional changes. The dynamic range analysis results (Fig. 7c) of the detected lipid species demonstrated that both the

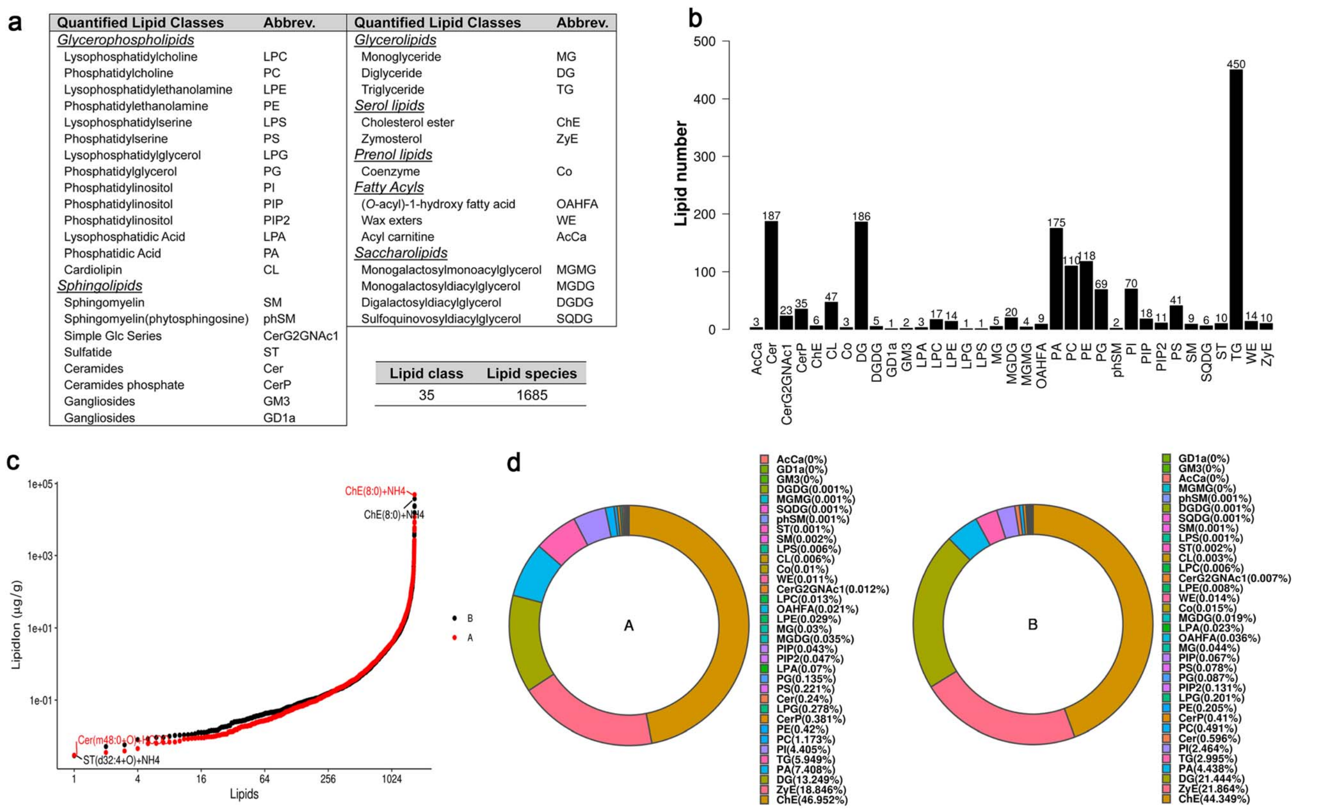

Fig. 7 The results of lipidome. Quantified lipid classes and their abbreviation (a and b). Dynamic range of identified and quantified lipids species, covering 6 orders of magnitude (c). The distribution of the different lipid classes in the control group (A pie) and I23-treated group (B pie).

control and the treated groups spanned a similar dynamic range, reflecting the less impacts on the lipid composition. Nevertheless, after treatment with **I23**, there were increases in the total proportions of sterol lipids (ChE and ZyE) and sphingolipids (Fig. 7d). Significantly, sterol lipids are thought to play a role in ensuring the stability of the lipid bilayer and resisting the permeabilization under osmotic stress.[44,45] Simultaneously, it is perceived that sphingolipids help stabilize the membrane bilayer.[46,47] Therefore, the increases might be the salvage response to the negative effects of **I23** on the cell membrane integrity and function of *P. recalcitrans*. Notably, glycerolipids are a large group of storage biological molecules necessary for membrane formation, metabolic energy, and fat acids in most living organisms.[48,49] In the present study, **I23** increased the proportion of glycerolipids, which might be also associated with different degrees of defects in membrane integrity and function.

The results of the lipid absolute quantification analysis (Fig. S5†) showed that **I23** could lead to the increase of the total lipid content but this difference did not reach significance. Notwithstanding, among the cell membrane components with the contents higher than 1%, Cer class, and PI and PC classes showed significant increase and decreases, respectively. To have a specific overview of how changes in the three lipid classes, the carbon chain length and the degree of unsaturation of the corresponding lipid species were further analyzed. As depicted in Fig. S6,† the Cer content enhanced at the different chain length and the degree of unsaturation levels, while PI and PC decreased. The alternation of Cer, PI and PC confirmed the instability and the integrity changes of the cell membrane induced by **I23**, which might be responsible for the malfunction and the increased permeability of cellular membrane *P. recalcitrans*. Besides, the 3D-QSAR analysis indicated that the hydrophobic R_1 and R_2 groups are favorable, suggesting the necessity of the hydrophobicity of the potent compounds. It has been demonstrated that the small hydrophobic molecules can easily enter into the cellular membranes, which might induce detrimental actions of **I23** on cellular membranes.

4. Conclusions

In conclusion, CCR was employed to synthesize a series of 3,4-dihydroisoquinolin-1(2*H*)-one derivatives as new antioomycete agents against *P. recalcitrans*. Compound **I23** showed the highest *in vitro* potency with an EC_{50} value of 14 μM, which was higher than the commercial hymexazol (37.7 μM). Moreover, **I23** exhibited the *in vivo* preventive efficacy of 75.4% at the dose of 2.0 mg per pot, which did not show significant differences with those of hymexazol treatments. When the dose was 5.0 mg per pot, **I23** achieved a preventive efficacy of 96.5%. The toxicity study indicated that the **I23** might exert the antioomycete activity *via* disruption of the biological membrane systems. In addition, the established CoMFA and CoMSIA models with reasonable statistics revealed the necessity of C4-carboxyl group and other structural requirements for activity. Therefore, our developed models can help to understand the SAR, and thus aid in the design and development of more potent 3,4-dihydroisoquinolin-1(2*H*)-one derivatives as antioomycete agents against *P. recalcitrans*. Design and synthesis of more new compounds are currently in progress.

Author contributions

D. Wang, Y. Fang, and Z. Zhang conceived the idea and designed the research. D. Wang, M. Li, and J. Li performed the research. M. Li, J. Li, Y. Fang, and Z. Zhang analyzed the data. D. Wang and M. Li wrote the original manuscript. Y. Fang, and Z. Zhang reviewed the manuscript. D. Wang was responsible for the funding acquisition.

Conflicts of interest

The authors declare that there are no conflicts of interest.

Acknowledgements

The study was supported by the National Natural Science Foundation of China (No. 31901909), and the Doctoral Research Startup Fund of Shanxi Agricultural University. The authors expressed gratitude to Professor Yan He, Northwest A&F University, for his molecular simulation in this work, and Professor Wang Tuhong, Institute of Bast Fiber crops, Chinese Academy of Agricultural Science, for identifying and providing the phytopathogen *Pythium recalcitrans*.

References

1 B. C. Gerwick and T. C. Sparks, *Pest Manage. Sci.*, 2014, **70**, 1169–1185.

2 C. L. Cantrell, F. E. Dayan and S. O. Duke, *J. Nat. Prod.*, 2012, **75**, 1231–1242.

3 F. E. Dayan, C. L. Cantrell and S. O. Duke, *Bioorg. Med. Chem.*, 2009, **17**, 4022–4034.

4 T. C. Sparks and S. O. Duke, *J. Agric. Food Chem.*, 2021, **69**, 8324–8346.

5 K. G. Meyer, K. Bravo-Altamirano, J. Herrick, B. A. Loy, C. Yao, B. Nugent, Z. Buchan, J. F. Daeuble, R. Heemstra, D. M. Jones, J. Wilmot, Y. Lu, K. DeKorver, J. DeLorbe and J. Rigoli, *Bioorg. Med. Chem.*, 2021, **50**, 116455.

6 R. Nauen, P. Jeschke, R. Velten, M. E. Beck, U. Ebbinghaus-Kintscher, W. Thielert, K. Wölfel, M. Haas, K. Kunz and G. Raupach, *Pest Manage. Sci.*, 2015, **71**, 850–862.

7 D. K. Yadav, N. Singh, K. Dev, R. Sharma, M. Sahai, G. Palit and R. Maurya, *Fitoterapia*, 2011, **82**, 666–675.

8 Y. Wang, D. Wang, J. Zhang, D. Liu, Z. Wang and D. Meng, *Phytochemistry*, 2018, **155**, 93–99.

9 A. Chiarugi, E. Meli, M. Calvani, R. Picca, R. Baronti, E. Camaioni, G. Costantino, M. Marinozzi, D. E. Pellegrini-Giampietro, R. Pellicciari and F. Moroni, *J. Pharmacol. Exp. Ther.*, 2003, **305**, 943.

10 R. K. Morgan, I. Carter-O'Connell and M. S. Cohen, *Bioorg. Med. Chem. Lett.*, 2015, **25**, 4770–4773.

11 R. Pellicciari, E. Camaioni, G. Costantino, L. Formentini, P. Sabbatini, F. Venturoni, G. Eren, D. Bellocchi, A. Chiarugi and F. Moroni, *ChemMedChem*, 2008, **3**, 914–923.

12 M. T. M. Nemr and A. M. AboulMagd, *Bioorg. Chem.*, 2020, **103**, 104134.
13 M. T. M. Nemr, M. Teleb, A. M. AboulMagd, M. E. El-Naggar, N. Gouda, A. A. Abdel-Ghany and Y. A. M. M. Elshaier, *J. Mol. Struct.*, 2023, **1272**, 134216.
14 S. Armstrong, J.-H. Li, J. Zhang and A. Rod Merrill, *J. Enzyme Inhib. Med. Chem.*, 2002, **17**, 235–246.
15 N. Jegham, M. B. Braiek, Y. Kacem and B. B. Hassine, *J. Chem. Res.*, 2016, **40**, 687–690.
16 A. R. Saundane, V. A. Verma and K. Vijaykumar, *Med. Chem. Res.*, 2013, **22**, 3787–3793.
17 V. V. Dabholkar and D. R. Tripathi, *J. Heterocycl. Chem.*, 2011, **48**, 529–532.
18 M. T. M. Nemr, A. M. AboulMagd, H. M. Hassan, A. A. Hamed, M. I. A. Hamed and M. T. Elsaadi, *RSC Adv.*, 2021, **11**, 26241–26257.
19 B. Dorothee, B. Emilie, C. Patrick, K. Mohamed, L. Pieter, N. Johan, M. Arnaud and V. Inge, US2011224208A1, 2011.
20 N. Guranova, D. Dar'in and M. Krasavin, *Synthesis*, 2018, **50**, 2001–2008.
21 A. Mikheyev, G. Kantin and M. Krasavin, *Synthesis*, 2018, **50**, 2076–2086.
22 P. J. Henry, H. R. George, L. S. Elizabeth, P. Albert, B. A. David, G. D. Eric and M. Michael, EP0247760A2, 1987.
23 S. W. Laws, S. Y. Howard, R. Mato, S. Meng, J. C. Fettinger and J. T. Shaw, *Org. Lett.*, 2019, **21**, 5073–5077.
24 E. Chupakhin, D. Dar' and M. Krasavin, *Tetrahedron Lett.*, 2018, **59**, 2595–2599.
25 V. Matyash, G. Liebisch, T. V. Kurzchalia, A. Shevchenko and D. Schwudke, *J. Lipid Res.*, 2008, **49**, 1137–1146.
26 M. A. Haimova, N. M. Mollov, S. C. Ivanova, A. I. Dimitrova and V. I. Ognyanov, *Tetrahedron*, 1977, **33**, 331–336.
27 N. Yu, L. Bourel, B. Deprez and J.-C. Gesquiere, *Tetrahedron Lett.*, 1998, **39**, 829–832.
28 S. Y. Howard, M. J. Di Maso, K. Shimabukuro, N. P. Burlow, D. Q. Tan, J. C. Fettinger, T. C. Malig, J. E. Hein and J. T. Shaw, *J. Org. Chem.*, 2021, **86**, 11599–11607.
29 Y. A. A. M. Elshaier, M. T. M. Nemr, M. S. Refaey, W. A. A. Fadaly and A. Barakat, *New J. Chem.*, 2022, **46**, 13383–13400.
30 A. Safrygin, O. Bakulina, D. Dar'in and M. Krasavin, *Synthesis*, 2020, **52**, 2190–2195.
31 C. Bian, S. Zhao, K. Jang and Y. Kang, *Australas. Plant Dis. Notes*, 2016, **11**, 7.
32 N. Li, Q. Zhou, K.-F. Chang, H. Yu, S.-F. Hwang, R. L. Conner, S. E. Strelkov, D. L. McLaren and G. D. Turnbull, *Crop Protect.*, 2019, **118**, 36–43.
33 L. Radmer, G. Anderson, D. M. Malvick, J. E. Kurle, A. Rendahl and A. Mallik, *Plant Dis.*, 2016, **101**, 62–72.
34 L. E. Berg, S. S. Miller, M. R. Dornbusch and D. A. Samac, *Plant Dis.*, 2017, **101**, 1860–1867.
35 E. Moralejo, A. Clemente, E. Descals, L. Belbahri, G. Calmin, F. Lefort, C. F. J. Spies and A. McLeod, *Mycologia*, 2008, **100**, 310–319.
36 X. H. Lu, R. Michael Davis, S. Livingston, J. Nunez and J. J. Hao, *Plant Dis.*, 2011, **96**, 384–388.
37 M. T. Kirkpatrick, J. C. Rupe and C. S. Rothrock, *Plant Dis.*, 2006, **90**, 592–596.
38 J. R. Lamichhane, M. P. You, V. Laudinot, M. J. Barbetti and J.-N. Aubertot, *Plant Dis.*, 2019, **104**, 610–623.
39 N. Guan and L. Liu, *Appl. Microbiol. Biotechnol.*, 2020, **104**, 51–65.
40 Y. Wang, Y. Sun, J. Wang, M. Zhou, M. Wang and J. Feng, *Plant Dis.*, 2019, **103**, 944–950.
41 S. C. Ricke, *Poult. Sci.*, 2003, **82**, 632–639.
42 P. J. Quinn, *Prog. Lipid Res.*, 2010, **49**, 390–406.
43 G. van Meer, D. R. Voelker and G. W. Feigenson, *Nat. Rev. Mol. Cell Biol.*, 2008, **9**, 112–124.
44 A. M. Farnoud, A. M. Toledo, J. B. Konopka, M. Del Poeta and E. London, in *Current Topics in Membranes*, ed. A. K. Kenworthy, Academic Press, 2015, vol. 75, pp. 233–268.
45 S. Dupont, L. Beney, T. Ferreira and P. Gervais, *Biochim. Biophys. Acta Biomembr.*, 2011, **1808**, 1520–1528.
46 L. V. Michaelson, J. A. Napier, D. Molino and J.-D. Faure, *Biochim. Biophys. Acta Mol. Cell Biol. Lipids*, 2016, **1861**, 1329–1335.
47 F. M. Goñi and A. Alonso, *Biochim. Biophys. Acta Biomembr.*, 2006, **1758**, 1902–1921.
48 D. R. Voelker, in *Encyclopedia of Biological Chemistry*, ed. W. J. Lennarz and M. D. Lane, Academic Press, Waltham, 2nd edn., 2013, pp. 412–418.
49 C.-L. E. Yen, S. J. Stone, S. Koliwad, C. Harris and R. V. Farese Jr, *J. Lipid Res.*, 2008, **49**, 2283–2301.